1816

MASTER

ORNL-4660
UC-25 – Metals, Ceramics, and Materials

MEASUREMENT AND CORRELATION OF THERMAL RESISTANCES OF UN-METAL INTERFACES

R. K. Williams
T. E. Banks
D. L. McElroy

OAK RIDGE NATIONAL LABORATORY
perated by
UNION CARBIDE CORPORATION
for the
U.S. ATOMIC ENERGY COMMISSION

BLANK PAGE

BLANK PAGE

ORNL-4660

Contract No. W-7405-eng-26

METALS AND CERAMICS DIVISION

MEASUREMENT AND CORRELATION OF THERMAL RESISTANCES OF UN-METAL INTERFACES

R. K. Williams, T. E. Banks, and D. L. McElroy

MAY 1971

OAK RIDGE NATIONAL LABORATORY
Oak Ridge, Tennessee
operated by
UNION CARBIDE CORPORATION
for the
U.S. ATOMIC ENERGY COMMISSION

CONTENTS

	Page
List of Symbols	iv
Abstract	1
Introduction	1
Apparatus	3
Samples	6
Results	8
Discussion	21
Stress	22
Time at Stress	23
Correlation Via Tien's Method	27
Conclusions and Recommendations for Future Work	34
Appendix A	39
Appendix B	47

LIST OF SYMBOLS

A = empirical constant in Eq. (8).

A' = empirical constant in Eq. (8) with $\delta = 1.0$.

A_a = geometrical contact area, cm^2, Eq. (6).

A_c = actual contact area, cm^2, Eq. (6).

H = Vickers microhardness (VHN) number, kg/mm^2.

N = number of materials, Eq. (4).

R_c = thermal contact resistance of one interface, $°C\ cm^2\ W^{-1}$, Eq. (1).

ΔT_i = temperature drop at one interface, Eq. (1).

ΔT_T = total temperature drop across two interfaces and one metal foil, Eq. (2).

a = radius of a circular solid-solid contact spot, Eq. (3).

b = empirical constant in Eq. (9).

d = empirical constant in Eq. (9).

f = multiplication factor in Eq. (11b). May be a function of the root-mean-square slope, m (Appendix B).

g = empirical constant in Eq. (9).

m = root-mean-square slope (see ref. 10 and Appendix B).

n = number of solid-solid contact spots per square centimeter, Eq. (5).

q = heat flux perpendicular to the test interface.

r_c = thermal resistance of one solid-solid contact, Eq. (3).

t = metal foil thickness (simulates cladding).

α = constant in Eq. (11).

β = constant in Eq. (11).

γ = root-mean-square surface roughness, cm.

γ_1 = root-mean-square surface roughness of material 1, cm.

δ = empirical constant in Eq. (8).

λ = thermal conductivity, $W\ cm^{-1}\ deg^{-1}$.

λ_m = harmonic mean thermal conductivity, Eq. (4).

ξ = proportionality constant in Eq. (6).

σ = compressive stress, psi or kg/mm^2, as noted.

MEASUREMENT AND CORRELATION OF THERMAL RESISTANCES OF UN–METAL INTERFACES

R. K. Williams, T. E. Banks,[1] and D. L. McElroy

ABSTRACT

We obtained data on thermal contact resistance for contact interfaces between UN and several other metals in vacuum at about 50°C: UN–In, UN–type 1100 Al, UN–Cu, UN–V-15% Cr-5% Ti, UN–Mo, UN–UN, and three UN–type 302 stainless steel interfaces. Many variables affected the results, and the correlation of the data showed the relative importance of stress, hardness, thermal conductivity, and surface topography. The correlation obtained from the data also suggests means for reducing thermal contact resistance in fuel elements; these possibilities are discussed.

INTRODUCTION

Thermal resistance associated with the interface between two structural members is very important in many engineering situations.[2] One such area is the design of high-performance plate- or rod-types of fuel elements for breeder reactors. In this application, carbide or nitride fuel has a relatively high thermal conductivity, λ, but the maximum permissible operating temperatures are considerably lower than for conventional oxide fuels. For a fuel element of given geometry, the maximum power density is governed by the thermal resistance of the fuel element and the acceptable temperature difference between the fuel center and coolant. The thermal resistance of a rod- or plate-type of fuel element is in turn composed of contributions from the cladding (minor)

---

[1]Present address: University of Louisville, Louisville, Kentucky.

[2]E. Fried, "Thermal Conduction Contribution to Heat Transfer at Contacts," p. 253 in Thermal Conductivity, vol. 2, ed. by R. P. Tye, Academic Press, London and New York, 1969.

and fuel and the interface between fuel and cladding. As the λ of fuels increases, the interfacial thermal resistance becomes an increasingly important design consideration, and any measures that reduce the interfacial thermal resistance will improve the power rating.

Conventional methods for controlling interfacial thermal resistance, such as liquid-metal, helium, or pressure bonding, have known limitations.[3,4] The goals of our work were to determine which factors were most important in determining the interfacial resistance between UN and potential cladding materials and thus show ways of minimizing the effect.

When two solid bodies are placed in contact, the actual area of solid-solid contact is usually only a small fraction of the area of geometrical contact.[4] Heat can be transferred across the interface by three principal mechanisms: thermal radiation across the voids, conduction and convection through any fluid filling the voids, and conduction through the spots of solid-solid contact. Liquid-metal or helium bonding enhances conduction and convection across the voids, and pressure bonding increases the conduction via solid-solid contacts. Since the solid-solid conduction forms an upper limit for the contact conductance, R_c^{-1}, and since a promising method for increasing heat transfer is to increase the solid-solid part of the conductance, we chose this component for study. The solid-solid part of R_c can be studied by performing experiments in vacuum and restricting the temperature at the interface to levels at which thermal radiation can be neglected.

Many variables are known to affect R_c (ref. 4), and contacts between dissimilar materials may be subject to additional complications.[5] The property is related to the actual area of contact, the number of contact spots per unit area, and the thermal conductivity of the contacting members.[4] Experimental studies have shown that stress, surface topography, surface deformation characteristics, corrosion films, and (indirectly) temperature have significant effects on the contact area

---

[3]J. W. Prados, private communication.

[4]M. L. Minges, Thermal Contact Resistance: A Review of the Literature, vol 1, AFML-TR-65-375 (April 1966).

[5]J. S. Moon and R. N. Keeler, Intern. J. Heat Mass Transfer 5, 967–971 (1962).

and the density of contact spots. The results we obtained on contacts between UN and metals allow an assessment of the relative importance of stress, thermal conductivity, and surface deformation characteristics. Surface topography certainly plays a significant role,[4] but time did not permit a quantitative assessment of its importance. Test conditions were chosen, however, to hold the root-mean-square (rms) surface roughness characteristics approximately constant.

APPARATUS

Determination of R_c involves measurement of the temperature drop between two surfaces, ΔT_i, and the heat flux perpendicular to the interface, q:

$$R_c = \frac{\Delta T_i}{q} \text{ (deg cm}^2 \text{ W}^{-1}) \ . \qquad (1)$$

Since R_c is not an intrinsic property, other variables must be measured for a reasonably complete description: sample characteristics, compressive stress at the interface, pressure of gases in the voids (vacuum), and the average temperature at the interface. A time dependence is also concealed in the sample characteristics, since plastic flow can produce irreversible surface changes.

The tests were conducted in a modified version of a comparative axial-flow thermal-conductivity device described by Moore et al.[6] In this technique, ΔT_i is obtained by measuring temperatures at several known positions along two rod samples, least-squares fitting the temperature-distance data to straight lines, and extrapolating to obtain the temperatures at the interface between the two samples. The heat flux is derived from the measured temperature gradients and experimental values for the λ of the rod samples.

---

[6] J. P. Moore, T. G. Kollie, R. S. Graves, and D. L. McElroy, Thermal Conductivity Measurements on Solids Between 20 and 150°C Using a Comparative-Longitudinal Apparatus: Results on MgO, BeO, ThO_2, $Th_xU_{1-x}O_{2+y}$ and Al-UO_2 Cermets, ORNL-4121 (June 1967).

Pressures of about 2 to 3 × 10^{-6} torr were routinely obtained in the apparatus, assuring elimination of fluid conduction and convection through all open pores.

A schematic diagram of the modified apparatus is shown in Fig. 1. Major alterations of the version described by Moore et al.[6] included the following:

1. The rigidity at the mechanical loading system was increased, and the O-ring feed-through was replaced with a bellows seal.

2. A calibrated Baldwin-Lima-Hamilton Type U1 load cell was inserted for determination of the compressive stress. The load cell was calibrated by replacing the sample column with a second calibrated

ORNL-DWG 71-1001

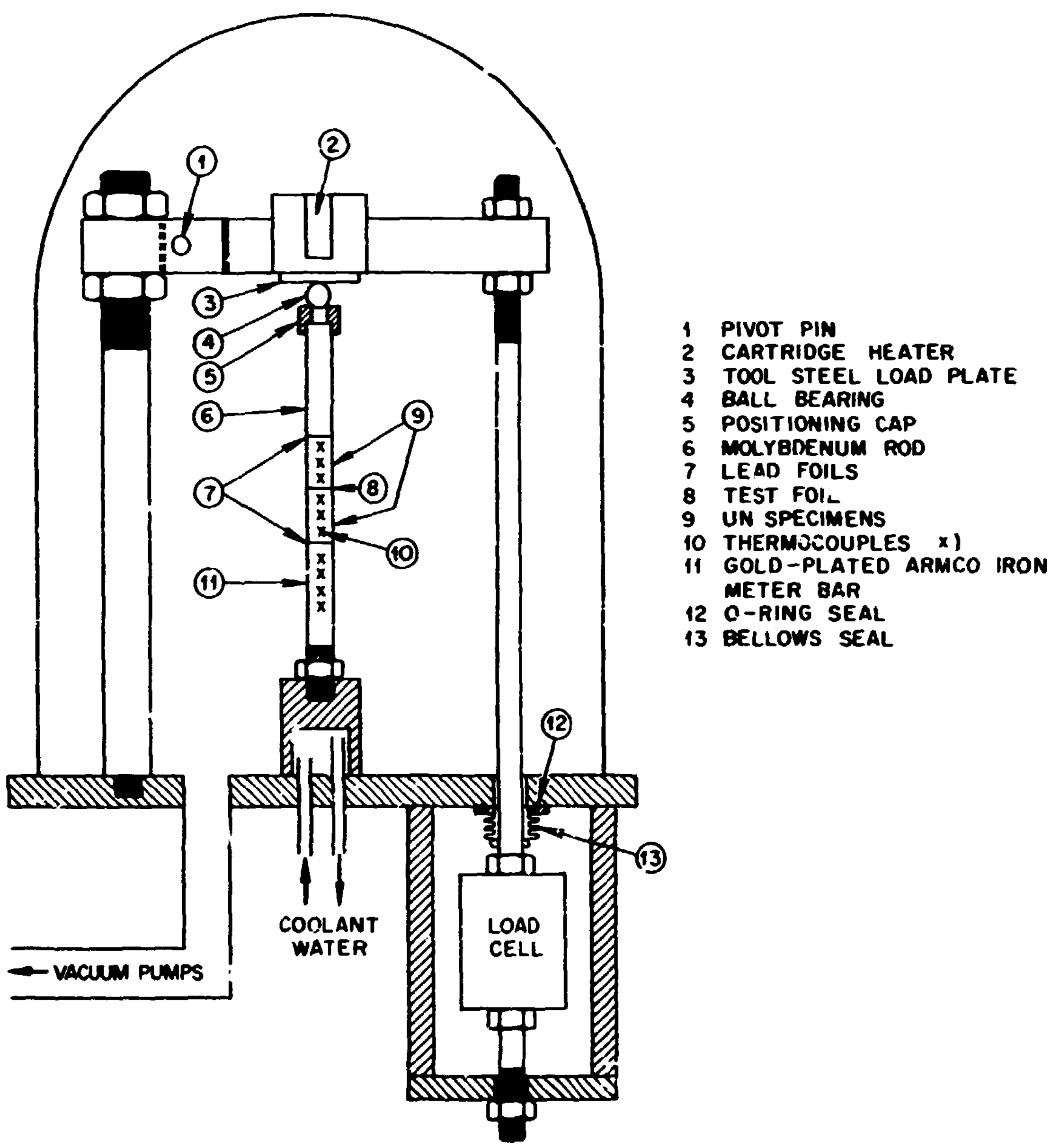

Fig. 1. Schematic View of Apparatus for Measuring Thermal Contact Resistance.

load cell and reading both load cells at several load levels. A correction for the load from the bellows feed-through was also determined experimentally.

3. Two UN samples and a metal foil, which was sandwiched between them, were included in the sample column. This part of the column simulated the interface between fuel (UN) and cladding (foil) in a fuel element. A molybdenum rod and an Armco iron bar and two thick (0.038 cm) lead foils were also included in the column, as shown in Fig. 1.

4. Extra Chromel-P vs Constantan thermocouples were attached to the two UN samples so that two independent R_c calculations could be made. The two rows of thermocouples were positioned 90° apart on the samples, and one row was aligned with the axis defined by the load arm. This arrangement was included because an anisotropic stress distribution across the UN-foil interface was sometimes encountered.

With the experimental arrangement shown in Fig. 1, the average contact resistance of one interface is given by:

$$R_c \equiv \frac{\Delta T_i}{q} = \frac{\Delta T_T}{2q} - \left(\frac{t}{\lambda}\right)_{foil} , \tag{2}$$

where

t = foil (cladding) thickness, and

ΔT_T = total temperature drop between the UN samples.

In these experiments, the conductive thermal resistance, t/λ, was usually 10% or less of the total resistance $\left(\frac{\Delta T_T}{q}\right)$. The heat flux values used for the calculation were obtained from the temperature gradient and the λ for the UN samples. The q value from the Armco iron meter bar was used as a secondary check. The q values usually indicated a progressive heat loss of 5 to 10% between the top UN specimen and the Armco iron meter bar; therefore, we used the average of the q values from the two UN samples in computing R_c.

The procedure for calculating the determinant error in the R_c values was discussed by Moore et al.[6] The errors arise from uncertainties in temperature measurement, thermocouple location, heat flux, t_{foil} and λ_{foil}; the total maximum determinant errors were calculated assuming

±0.1°C, ±6.35 × 10^{-3} cm, ±0.05 q, ±2.54 × 10^{-4} cm, and ±0.15 λ_{foil} for these respective uncertainties. These calculations showed that the R_c values were usually uncertain to about ±10 to 20% at R_c levels of 5 to 10 deg cm^2 W^{-1}. Error bands shown with the R_c data correspond to the calculated maximum determinant error.

Uncertainty in the compressive stress, σ, was also a source of error. The calibrations of the load cell showed that the loading and unloading curves consistently differed by about 100 psi. The stresses were calculated from the average of the two curves, and are, therefore, uncertain to at least ±50 psi. Additional uncertainty from the calibration of the load cell amounted to about ±10 psi; therefore, the stress values are probably uncertain to about ±60 psi.

SAMPLES

The two UN samples were prepared by pressing and sintering UN powder.[7] These samples were ground to final size (2.54 cm long × 1.270 cm in diameter), and the two heat-transfer surfaces were lapped flat on a glass plate. The surface appearance of the UN samples is shown in Fig. 2. Profilometer measurements indicated an rms surface roughness of 1.5 to 2.0 × 10^{-5} cm for all heat-transfer surfaces. Vickers microhardness (VHN) tests at a 50-g load on a companion sample yielded a value of 649 kg/mm^2 (ref. 8). Measurements of immersion density indicated that the samples were 95.8% of theoretical density. Other characteristics of the samples were presented by Scarbrough et al.[9] The thermal conductivity of both UN samples was determined in the original[10] comparative heat-flow apparatus; these data are shown in Fig. 3.

---

[7] H. L. Whaley, W. Fulkerson, and R. A. Potter, J. Nucl. Mater. 31, 345 (1969).

[8] W. Fulkerson, private communication.

[9] J. O. Scarbrough, H. L. Davis, W. Fulkerson, and J. O. Betterton, Jr., Phys. Rev. 176, 666 (1968).

[10] J. P. Moore, T. G. Kollie, R. S. Graves, and D. L. McElroy, Thermal Conductivity Measurements on Solids Between 20 and 150°C Using a Comparative-Longitudinal Apparatus: Results on MgO, BeO, ThO_2, $Th_xU_{1-x}O_{2+y}$ and Al-UO_2 Cermets, ORNL-4121 (June 1967).

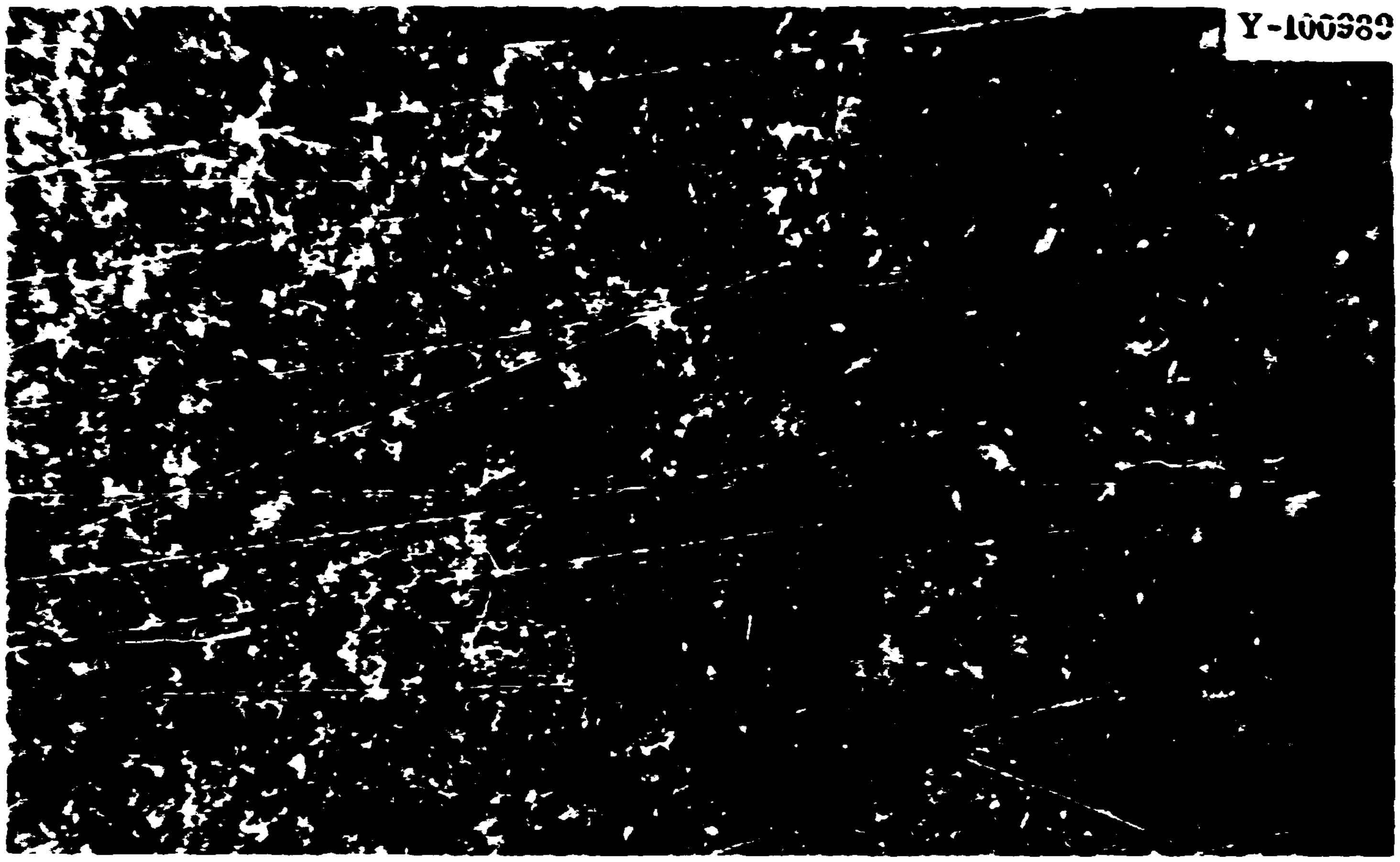

Fig. 2. Surface of Bottom UN Sample. Oblique light. 150×.

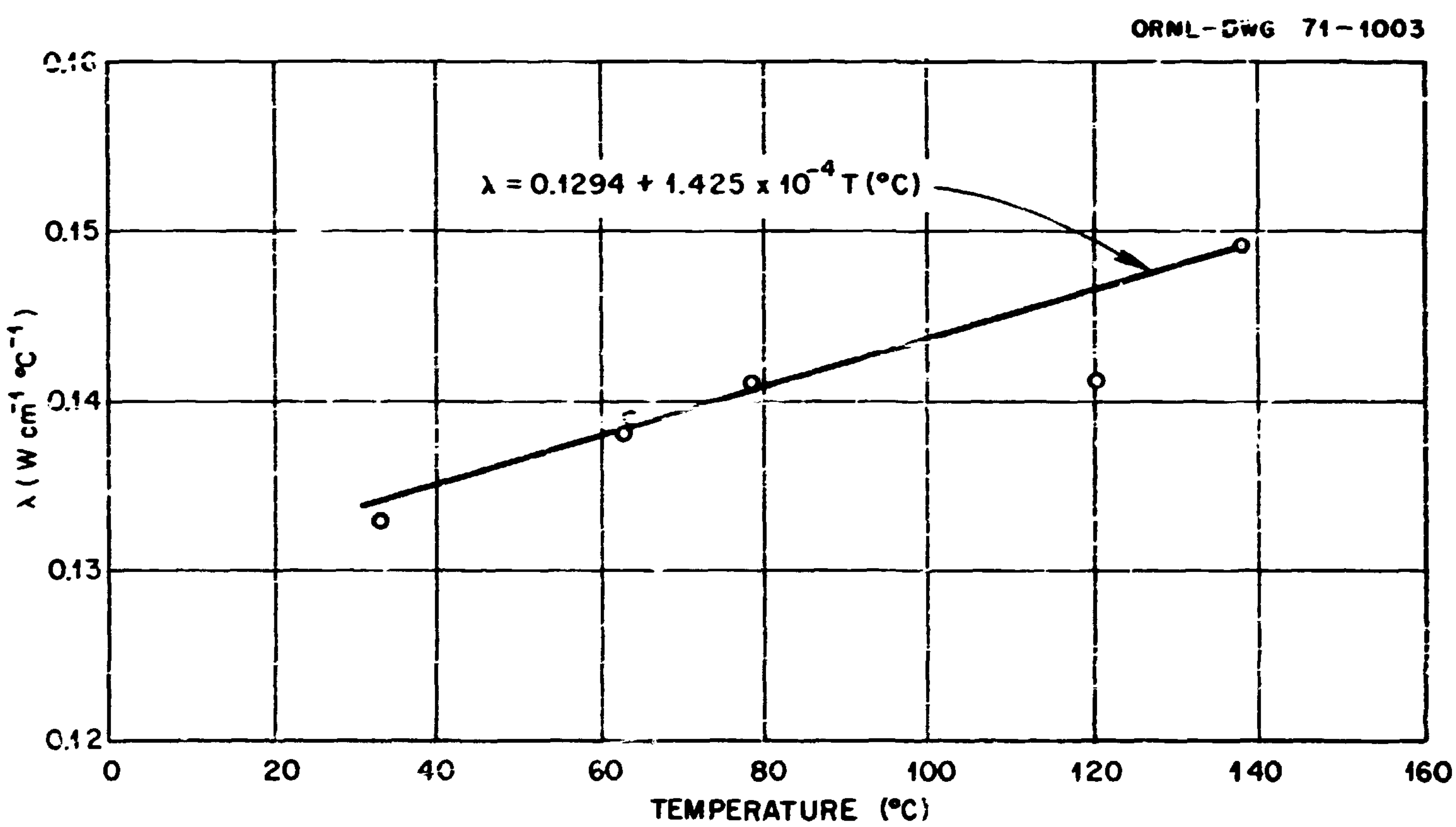

Fig. 3. Thermal Conductivity of UN Samples (95.8% of Theoretical Density) Used for Contact Resistance Studies. No porosity correction.

Characteristics of the eight metal foil (cladding) samples are shown in Table 1. In addition, values measured for electrical resistivity of the three stainless steel foils are shown in Table 2. The latter results were obtained to check for a possible variation in λ among the three stainless steel samples and do not indicate an important effect. The effect of load (25, 50, and 100 g) on measured microhardness values was also determined for the three stainless steel samples and the copper foil. None of these tests showed a significant dependence of hardness on test load between 25 and 100 g.

Photomicrographs of the surfaces of the foil samples are shown in Figs. 4 through 11. Except for the copper sample, which had been etched in dilute HNO_3, all of the foils had surfaces characterized by parallel ridges and valleys. This type of surface is usually obtained from the surface imperfections on a rolling mill. The 1100 aluminum foil showed evidence of plastic deformation and improvement of the surface finish during the R_c test. Counts of the relative density of ridges are included in Table 1.

RESULTS

Experimental data from nine runs are tabulated in Appendix A. These tabulations explain the time-temperature-stress sequence for data from each run. Some data were discarded because the mechanical loading system frequently produced an anisotropic stress distribution at the test interface. The failure could readily be detected by comparing the two independent R_c values, which were calculated from each set of steady-state data. The two values usually agreed well (i.e., within the combined maximum determinant errors) at low (300 to 1000 psi) stresses, but their ratio frequently showed a systematic deviation from unity as the stress was increased further. Data were rejected when the ratio of the two R_c values lay outside the range 0.80 to 1.20. For low (about 300 psi) stresses, this criterion approximately corresponds to the combined maximum determinant error, but at high stresses, where R_c is smaller, it is much less than the calculated error. The apparent inconsistency of discarding data for high stress, which disagree by less than

Table 1. Properties of Materials Used in Tests of Interfacial Resistance

Material	Thermal Conductivity at 50°C ($W\ cm^{-1}\ deg^{-1}$)	Root-Mean-Square Surface Roughness, cm		Vickers Hardness at 50-g Load (kg/mm^2)		Density of Ridges (lines/cm)		Thickness of Sample (cm)	Remarks
		Before	After	Before	After	Before	After		
		$\times 10^{-5}$	$\times 10^{-5}$						
Indium	0.758[a]			0.87[a]				0.0127	
1100 aluminum	2.29	2.0	1.4	27	30	1324	994	0.0127	
Copper	3.90		1.2		63			0.0107	Annealed 2 hr at 250°C in H_2. Light HNO_3 etch.
Annealed type 302 stainless steel	0.159	1.9	2.0		200	1565	1486	0.0127	
V-15% Cr-5% Ti alloy	0.15[b]	1.1	1.1	203	230	930	876	0.0127	Argonne National Laboratory Metallurgy Division Fabrication Technology Group. Item 282.
Molybdenum	1.10	1.0	0.8	329	321	1122	1033	0.0076	
Half-hard type 302 stainless steel	0.156	1.5	1.5		378	1161	1201	0.0127	
Full-hard type 302 stainless steel	0.153	1.2	1.2		458	950	891	0.0076	
UN	0.137	1.8		649[c]					

[a] M. Barisoni, R. K. Williams, and D. L. McElroy, "Physical Properties of Indium from 77 to 350 K," pp. 279–292 in Thermal Conductivity, Proc. 7th Conf. Gaithersburg, Maryland, Nov. 13–16, 1967, Nat. Bur. Std. Spec. Publ. 302, ed. by D. R. Flynn and B. A. Peavy, Jr., National Bureau of Standards, Washington, D.C., September 1968.

[b] Based on data for V-20 wt % Ti, R. J. Dunworth, Annual Progress Report for 1965: Metallurgy Division, ANL-7155, p. 36.

[c] W. Fulkerson, Oak Ridge National Laboratory, private communication.

Table 2. Electrical Resistivity Data and Thermal Conductivity Estimates for Type 302 Stainless Steel Samples

Mill Designation	Number of Samples	Average Electrical Resistivity[a] ($\mu\Omega$-cm)	Estimated Thermal Conductivity[b] (W cm^{-1} deg^{-1})	Remarks
Annealed	1	70.5	0.159	
Half hard	2	72.8_5	0.156	Weakly ferromagnetic
Full hard	3	74.8	0.153	Ferromagnetic

[a]Average cross-sectional area obtained by weighing sample, measuring total length (2.5 to 5.0 cm), and assuming a density of 7.9? g/cm^3.

[b]Calculated from $\lambda = \frac{L_0 T}{\rho} + 0.056$, where $L_0 = 2.443 \times 10^{-8}$ V^2 deg^{-2}; T = temperature, kelvins; ρ = Ω-cm.

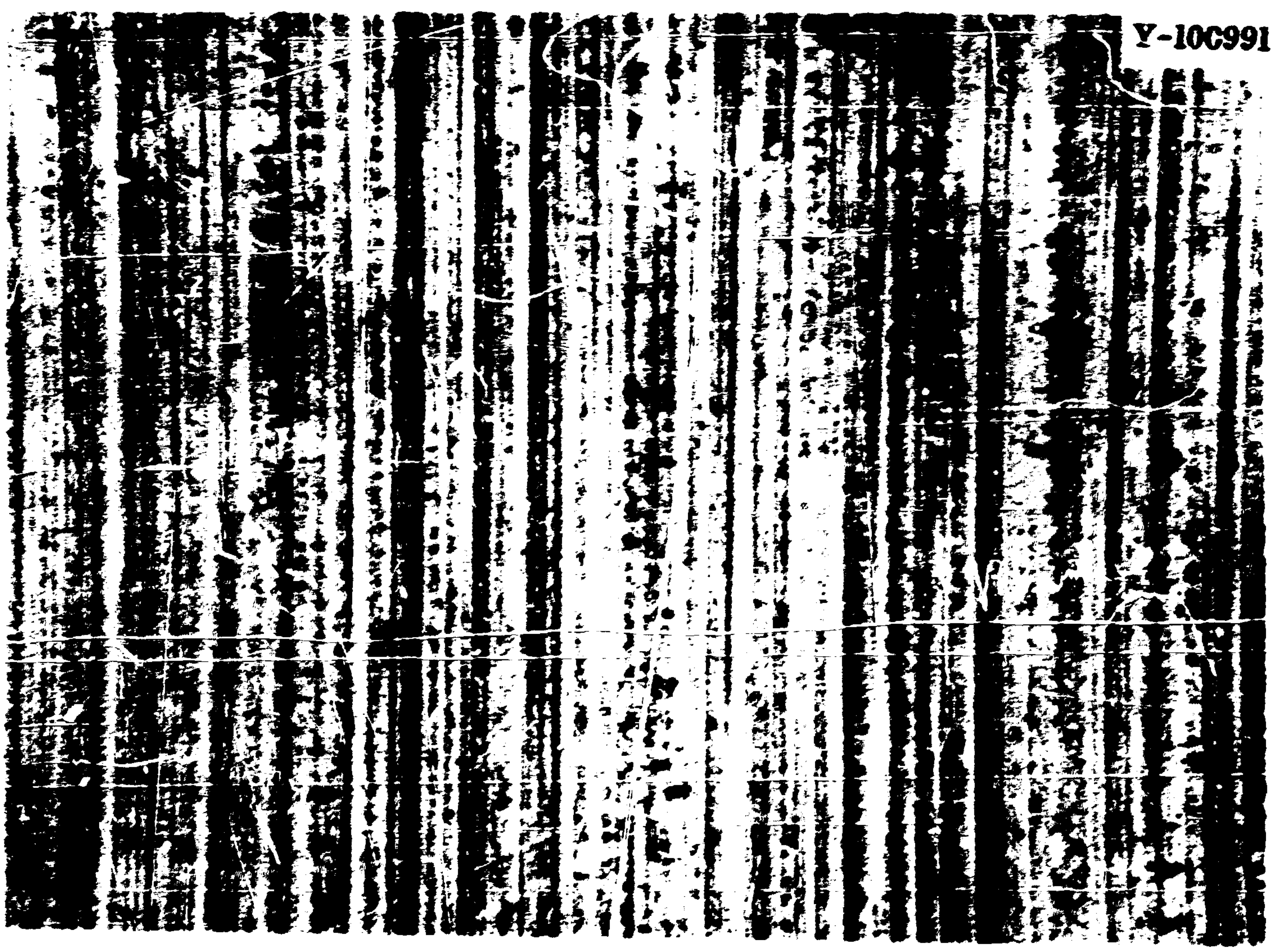

Fig. 4. Surface of 1100 Aluminum Sample Before Testing. Oblique light. 150×.

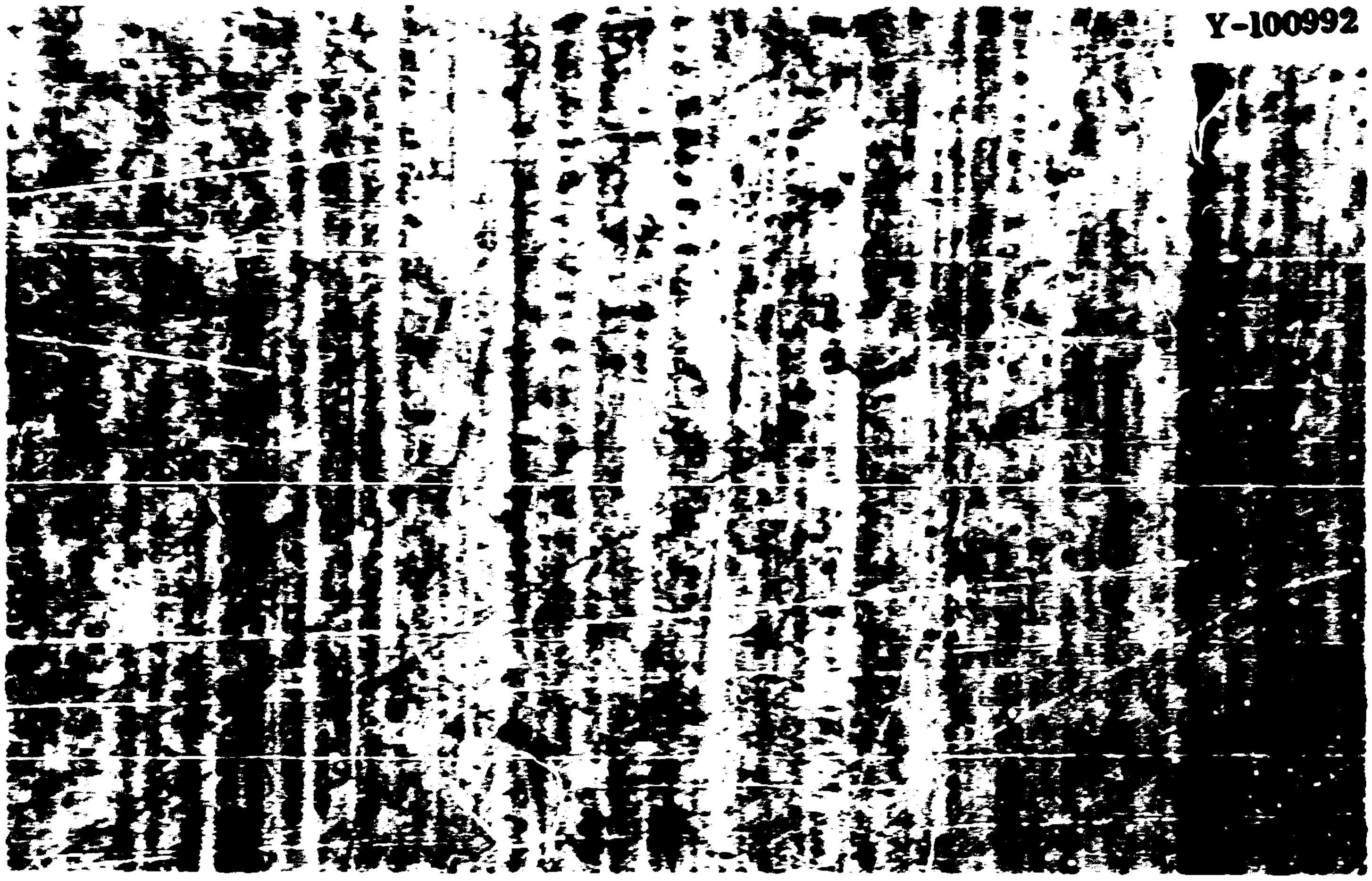

Fig. 5. Surface of 1100 Aluminum Sample After Testing. Oblique light. 150X.

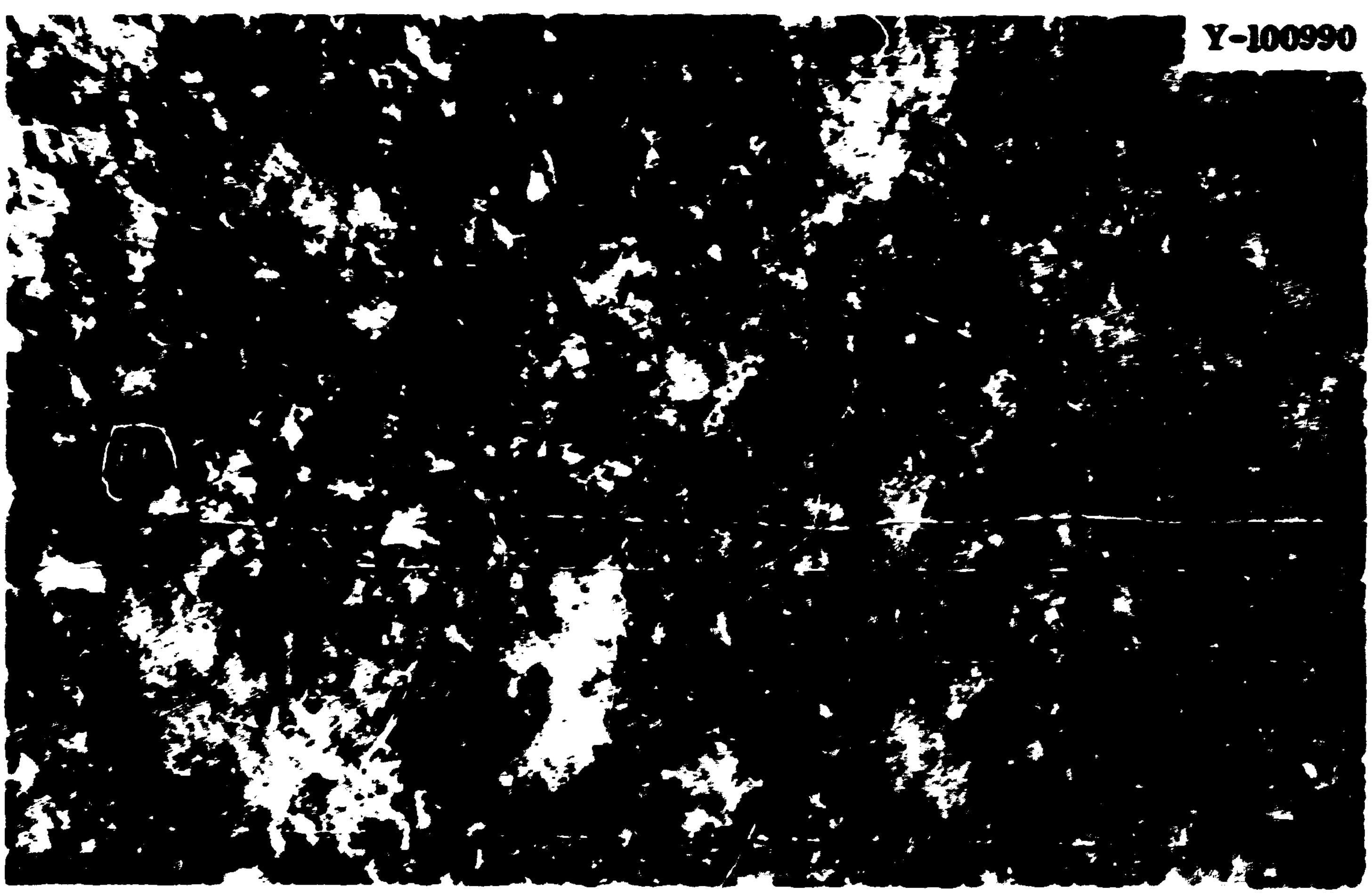

Fig. 6. Surface of Etched Copper Sample After Testing. Oblique light. 150X.

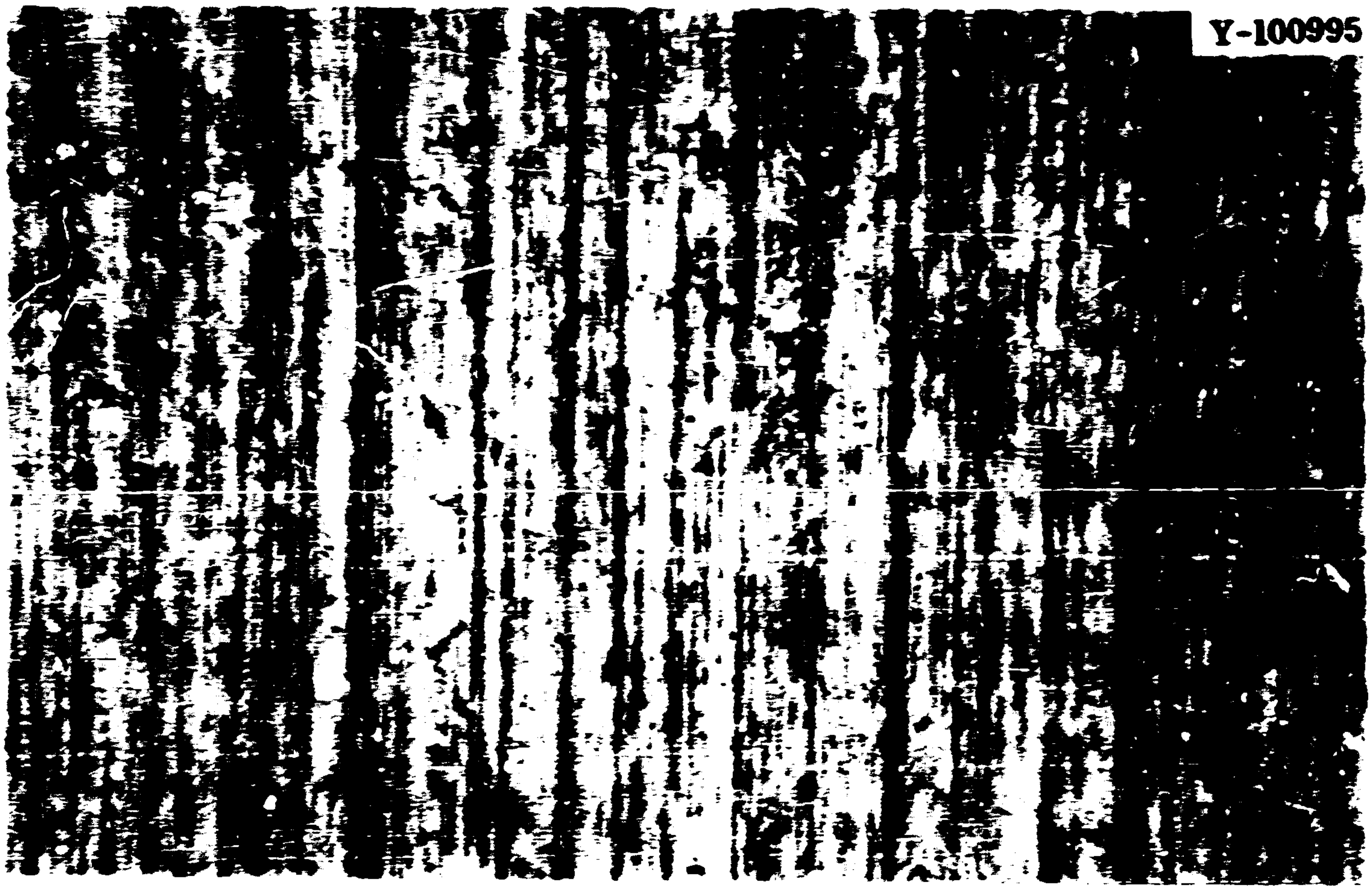

Fig. 7. Surface of Annealed Type 302 Stainless Steel Sample After Testing. Oblique light. 150×.

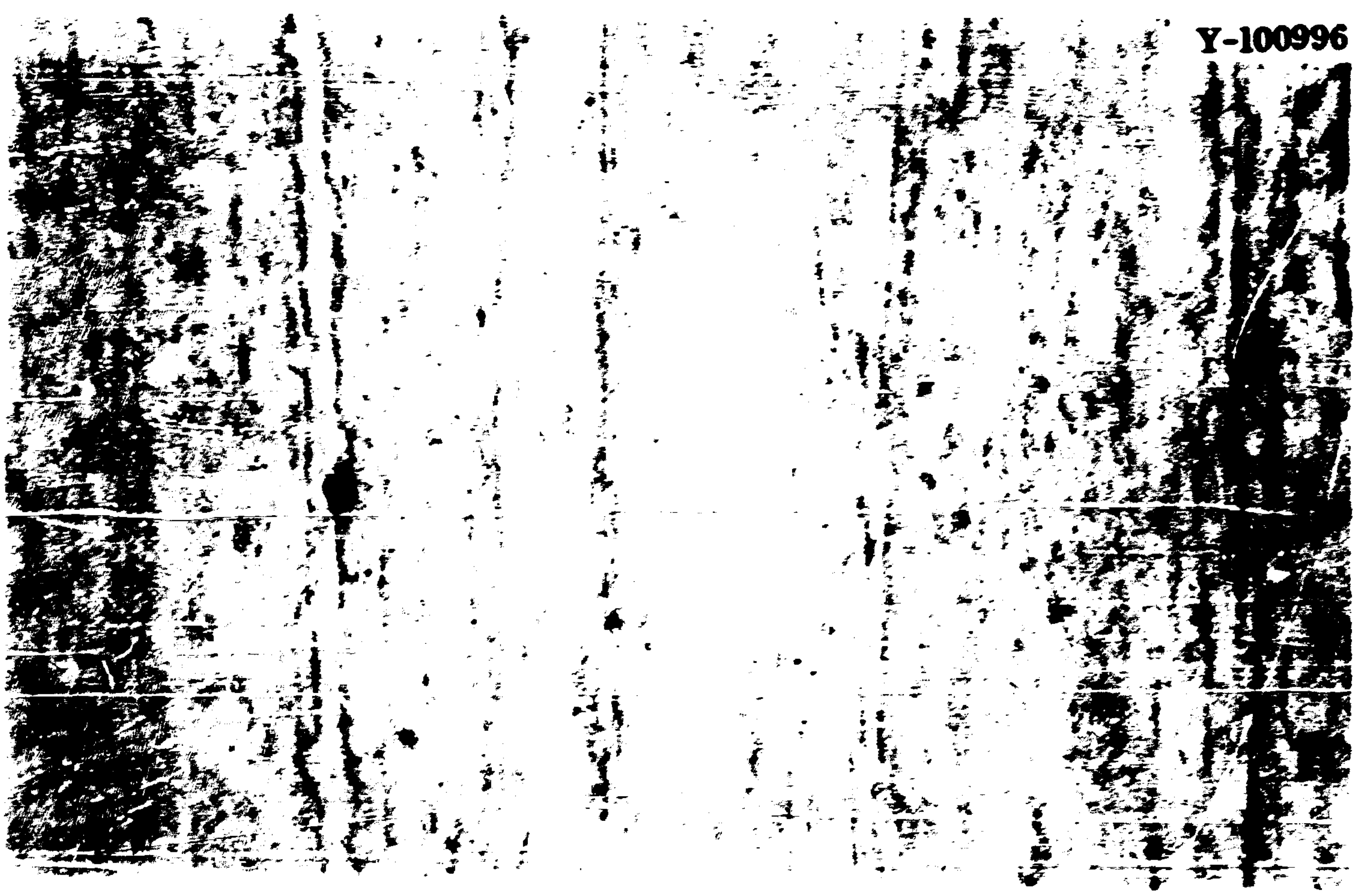

Fig. 8. Surface of V-15% Cr-5% Ti Sample After Testing. Oblique light. 150×.

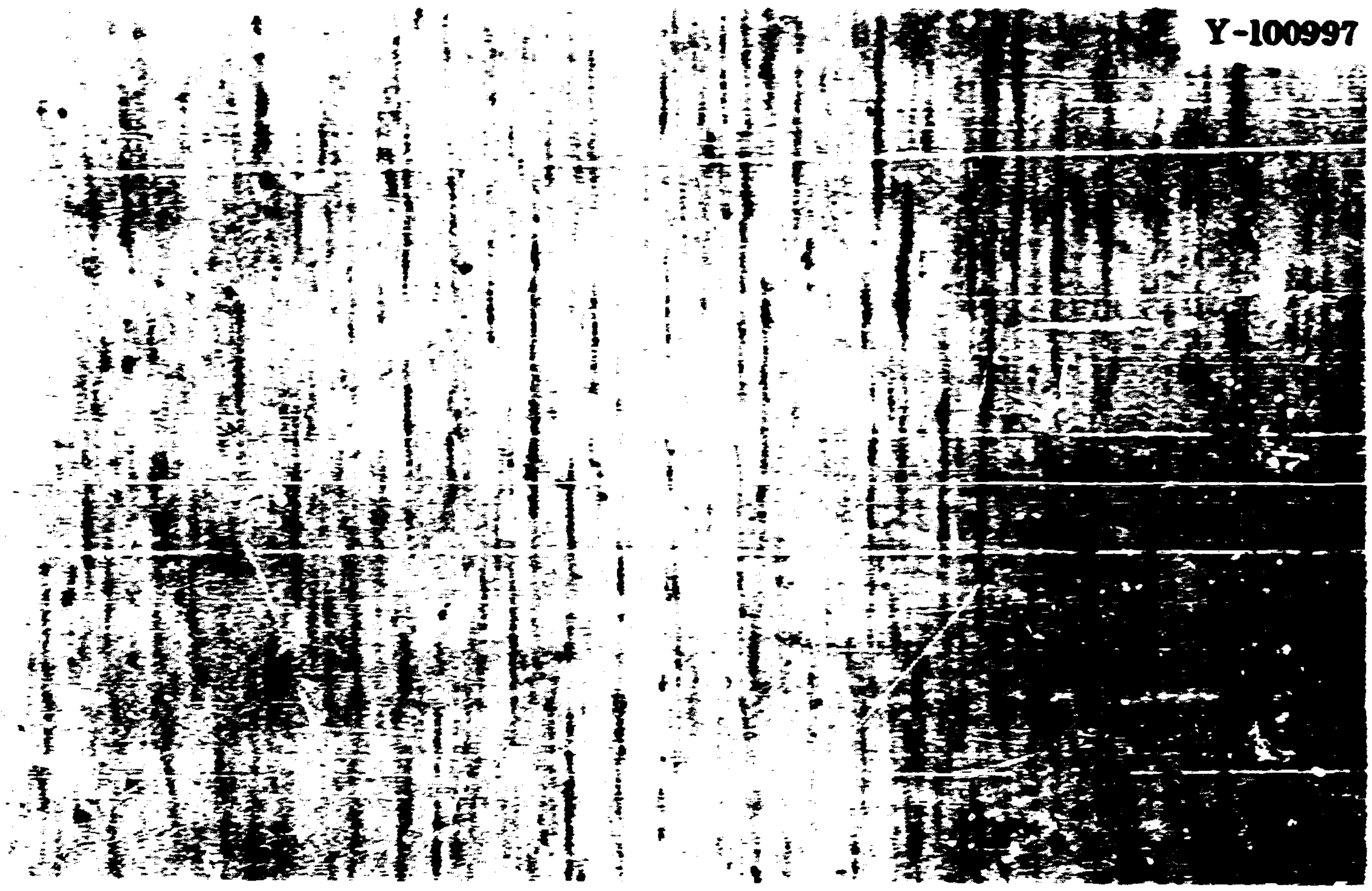

Fig. 9. Surface of Molybdenum Sample After Testing. Oblique light. 150×.

Fig. 10. Surface of Half-Hard Type 302 Stainless Steel Sample After Testing. Oblique light. 150×.

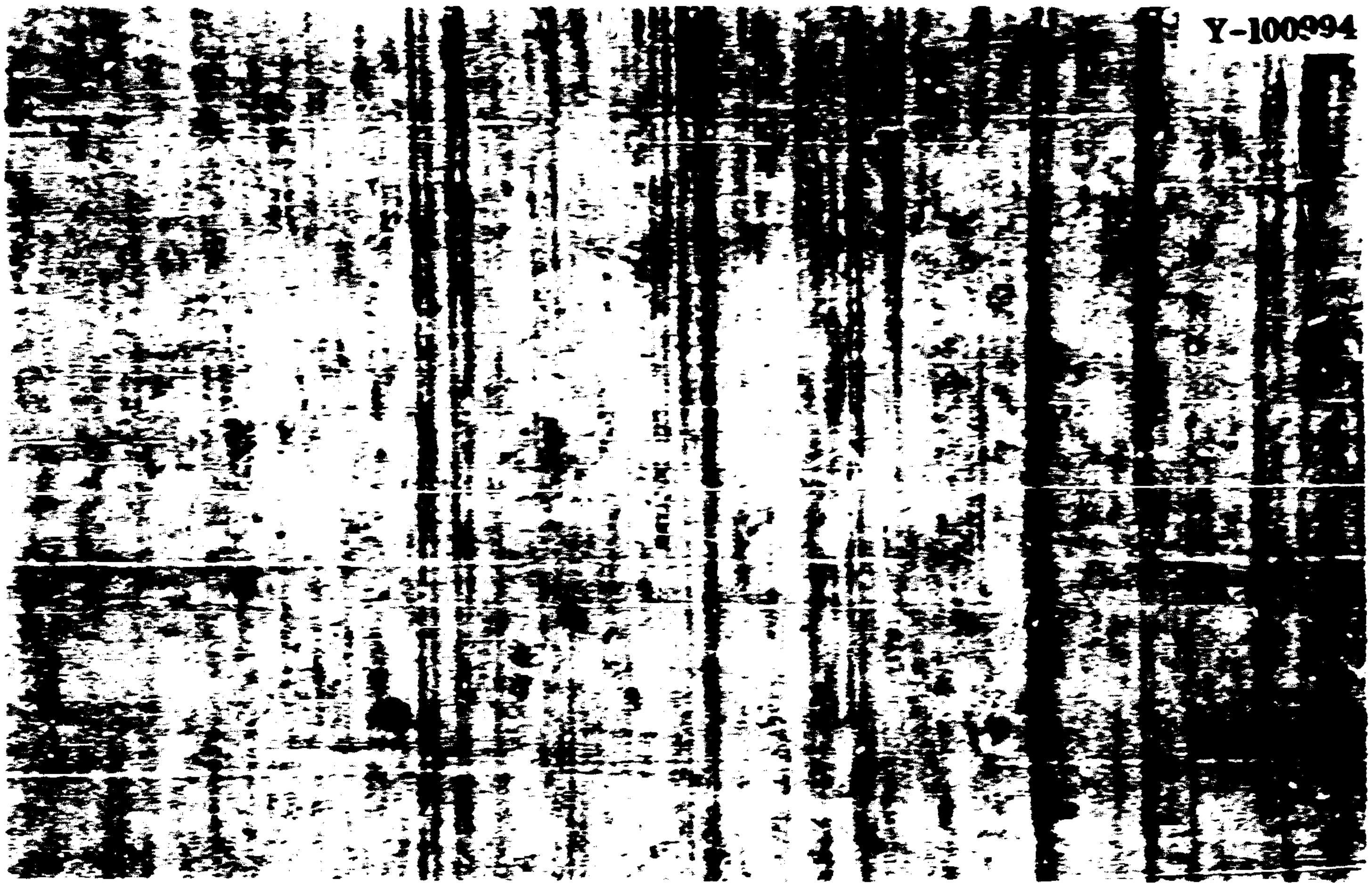

Fig. 11. Surface of Full-Hard Type 302 Stainless Steel Sample After Testing. Oblique light. 150×.

the combined experimental errors, is removed by considering two facts. First, the deviations nearly always took place gradually and always in the same nonrandom fashion as the stress was increased. This observation indicated nonuniform heat flow at the test interface. Second, since the R_c values obtained at high stresses ($R_c \approx 0.5$ deg cm^2 W^{-1}) were uncertain by nearly ±100%, they added little to the study.

The test temperatures should have had some effect on the R_c values, either through a small amount of radiation transfer or softening of the cladding. Several attempts (for interfaces of UN with In, Al, Cu, annealed type 302 stainless steel, V-15% Cr-5% Ti, and UN) were made to determine the effect, but test time (stress hysteresis) effects usually intervened. Also, the time response of the test column was too sluggish to allow experimental adjustment of all data to a common temperature. Fortunately, all tests indicated that temperature effects were small; and, in any case, most of the data were taken within ±20 deg of 50°C, so only small corrections for temperature effects were required.

The R_c data for all of the interfaces and at all stress levels were corrected to 50°C by means of data obtained on the interface of UN with annealed type 302 stainless steel. These results are shown in Fig. 12. These data were obtained by running the cartridge heaters (Fig. 1) at their power limits and adding additional radiation shielding around the load arm. Since it was necessary to replace several thermocouples after this series of tests, we did not consider repeating the measurements in the extended temperature range with other foils and at other stress levels to be justified. The data shown in Fig. 12 indicate a temperature coefficient of about −0.7%/deg near 50°C; we assumed this coefficient to be valid for our computations of all of the $R_c^{50°C}$

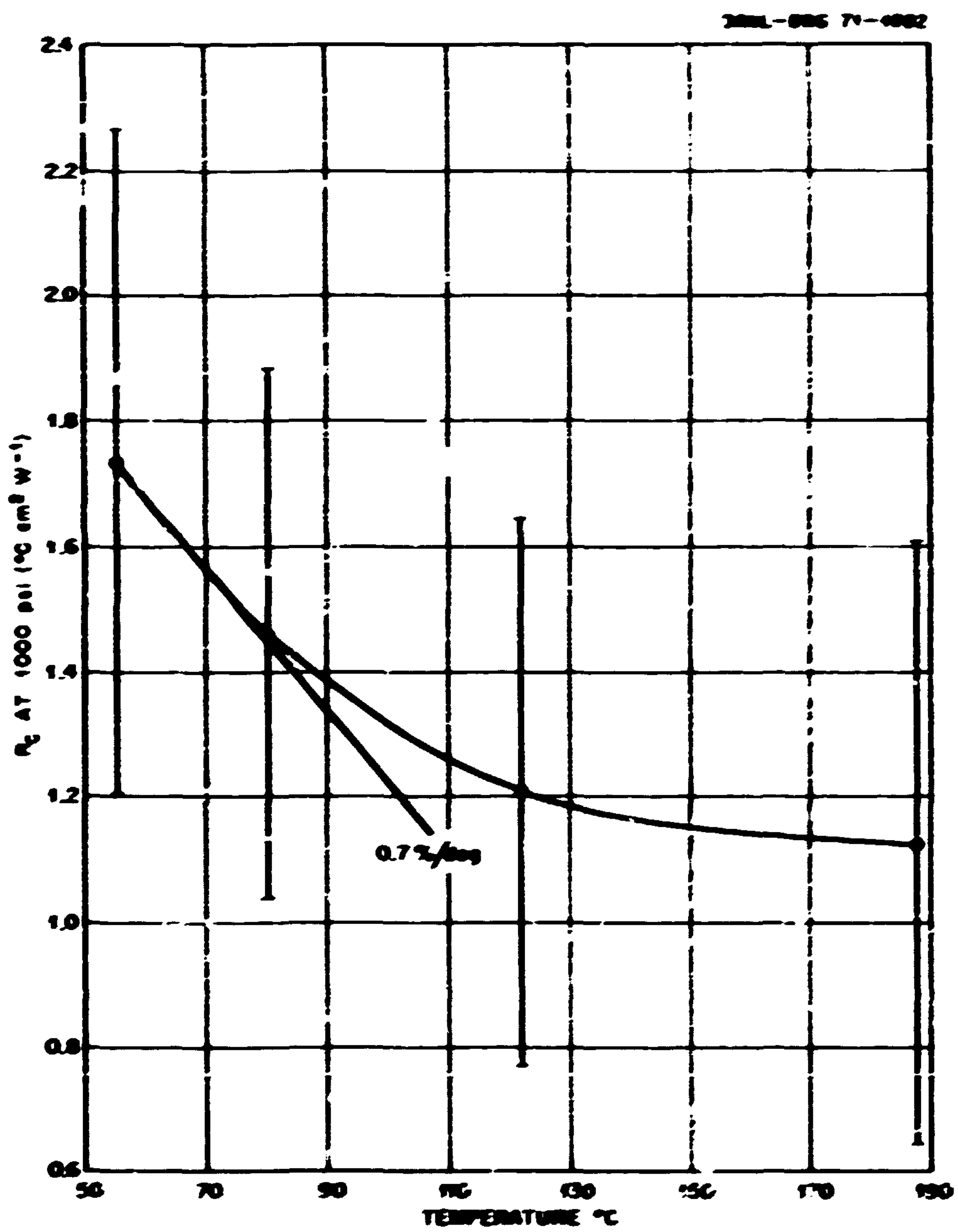

Fig. 12. Effect of Interface Temperature on R_c of Interface Between UN and Annealed Type 302 Stainless Steel at 1000-psi Compressive Stress.

values shown in Appendix A. Figures 13 to 21 show the $R_c^{50°C}$ values for individual runs plotted as a function of compressive stress. The error bands included for representative points are the maximum determinant error calculated from a conventional error analysis.[11]

[11] J. P. Moore, T. G. Kollie, R. S. Graves, and D. L. McElroy, Thermal Conductivity Measurements on Solids Between 20 and 150°C Using a Comparative-Longitudinal Apparatus: Results on MgO, BeO, ThO_2, $Th_xU_{1-x}O_{2+y}$ and $Al-UO_2$ Cermets, ORNL-4121 (June 1967).

ORNL-DWG 71-1004

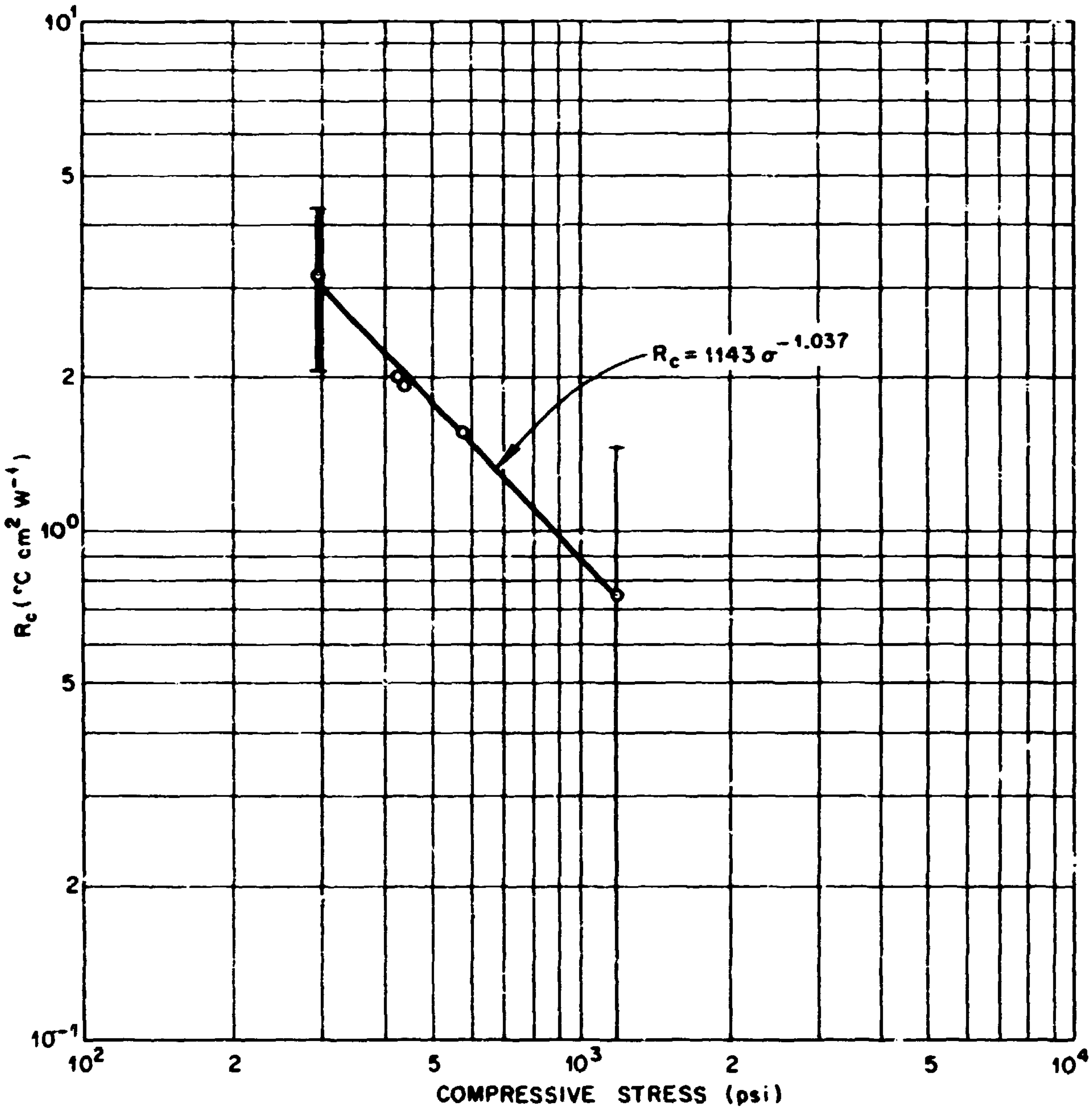

Fig. 13. Thermal Contact Resistance Data (50°C) for Interface Between UN and Indium.

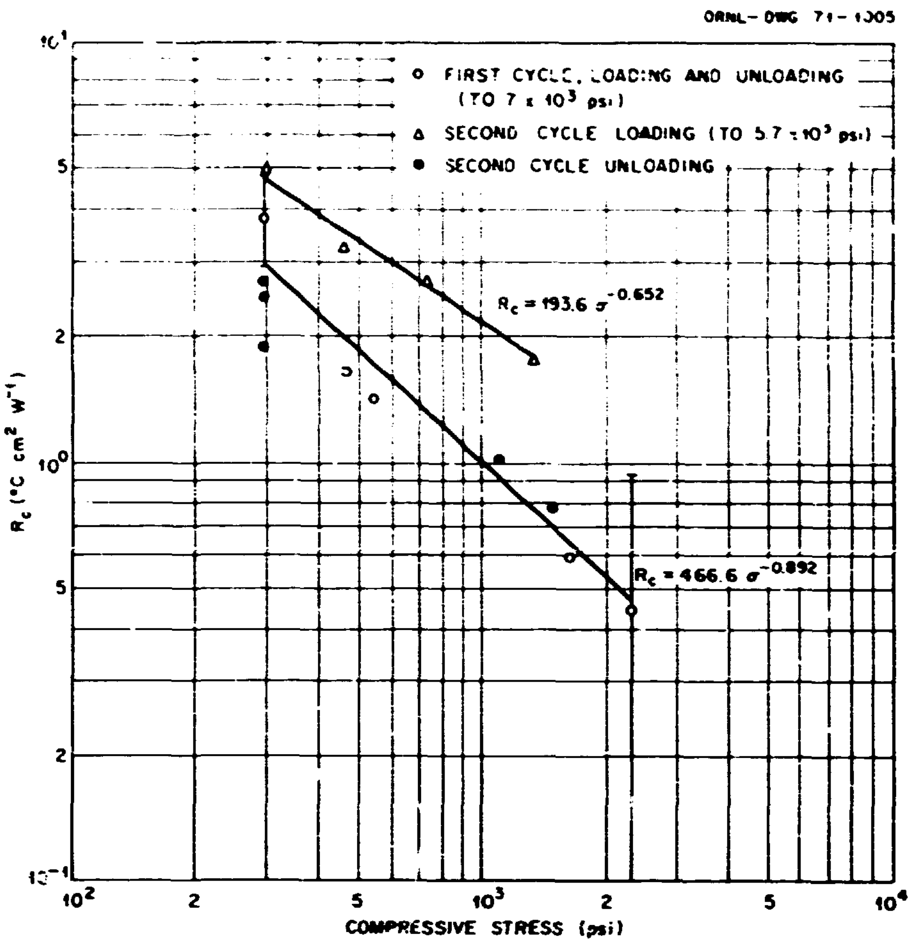

Fig. 14. Thermal Contact Resistance Data (50°C) for Interface Between UN and Type 1100 Aluminum.

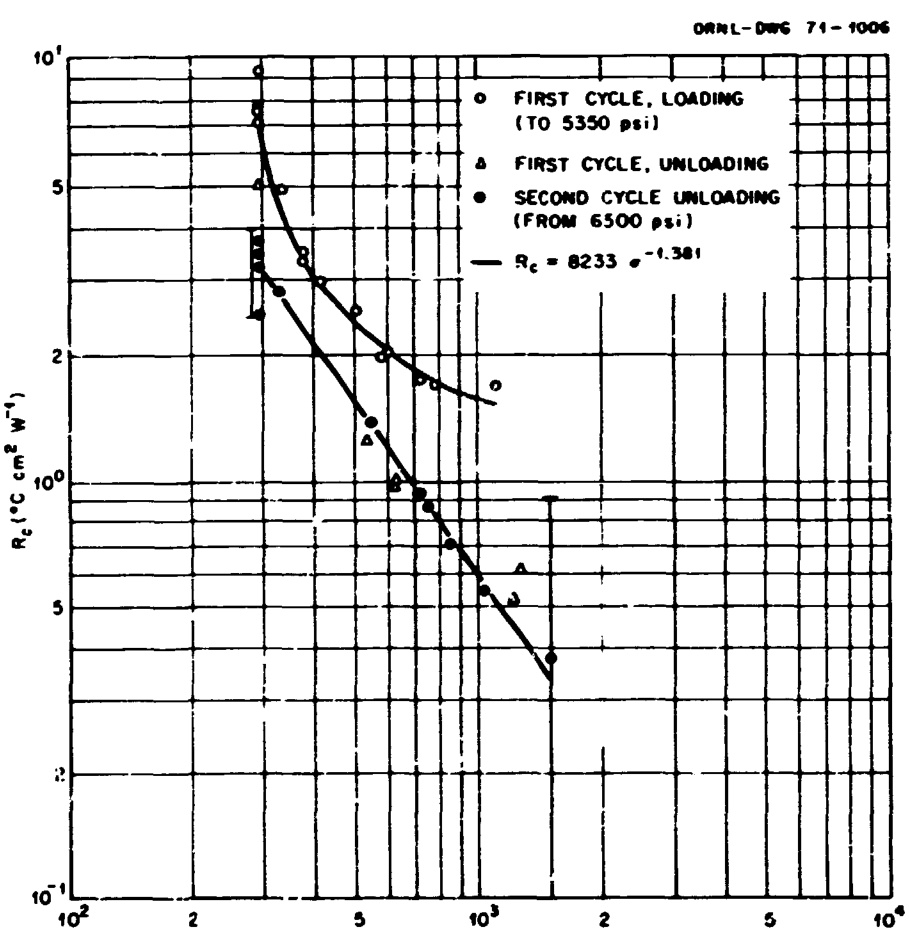

Fig. 15. Thermal Contact Resistance Data (50°C) for Interface Between UN and Copper.

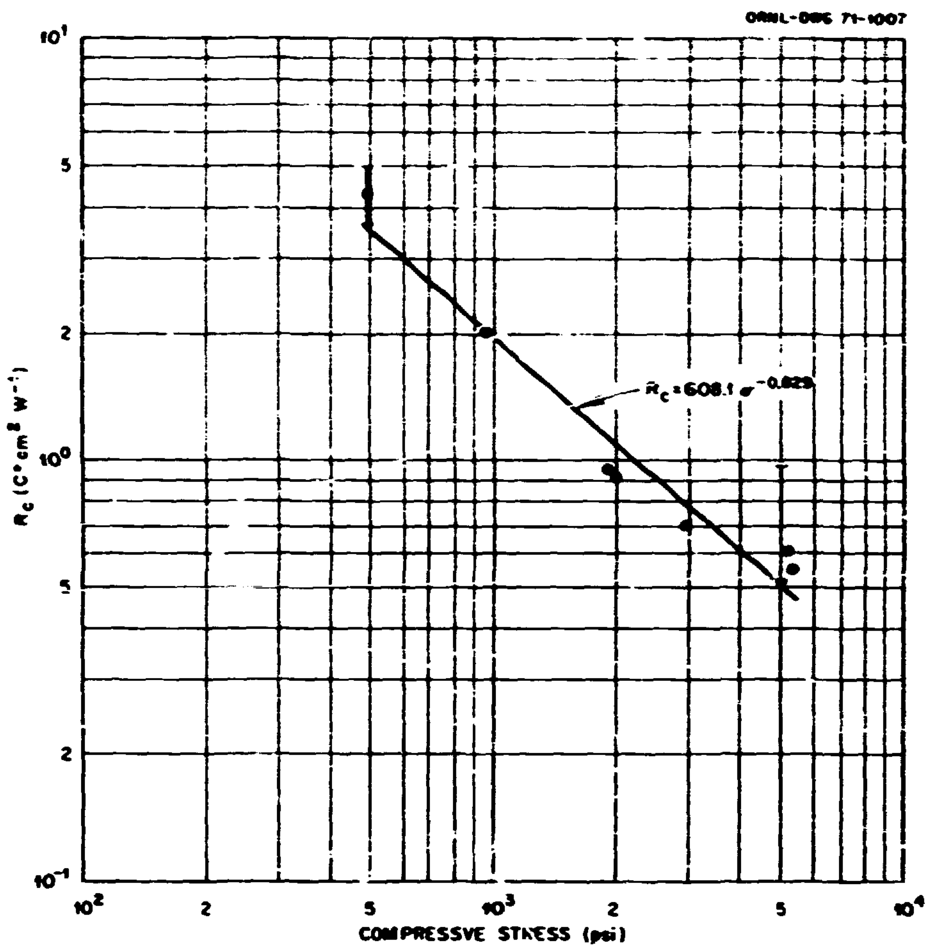

Fig. 16. Thermal Contact Resistance Data (50°C) for Interface Between UN and Annealed Type 302 Stainless Steel.

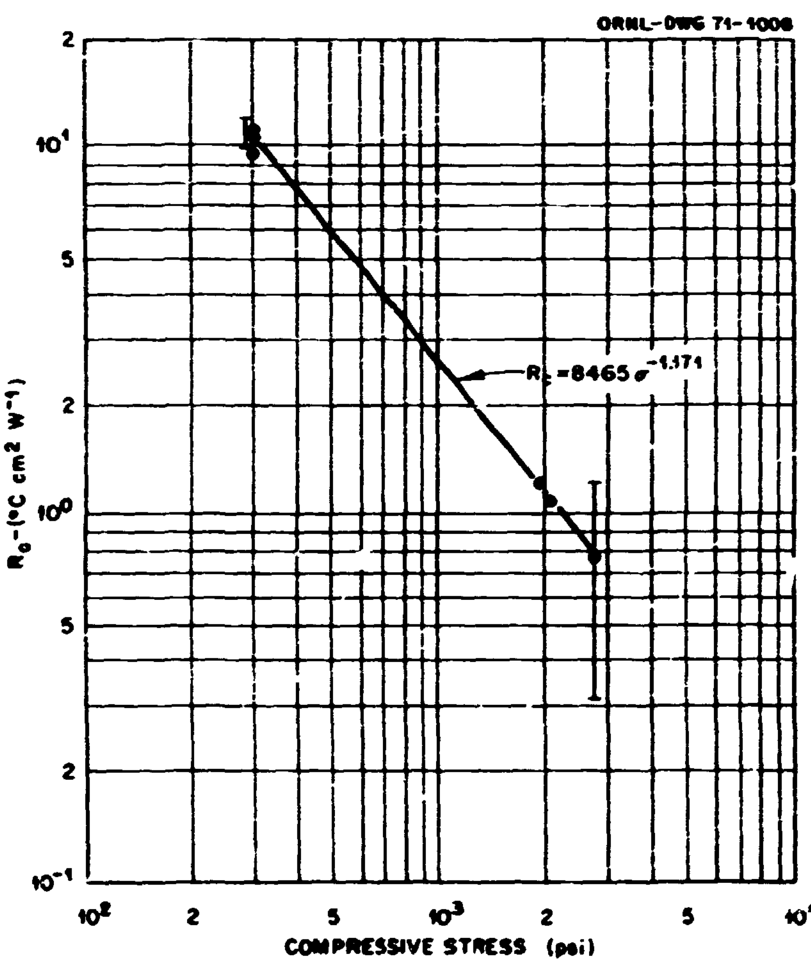

Fig. 17. Thermal Contact Resistance Data (50°C) for Interface Between UN and V–15% Cr–5% Ti Alloy.

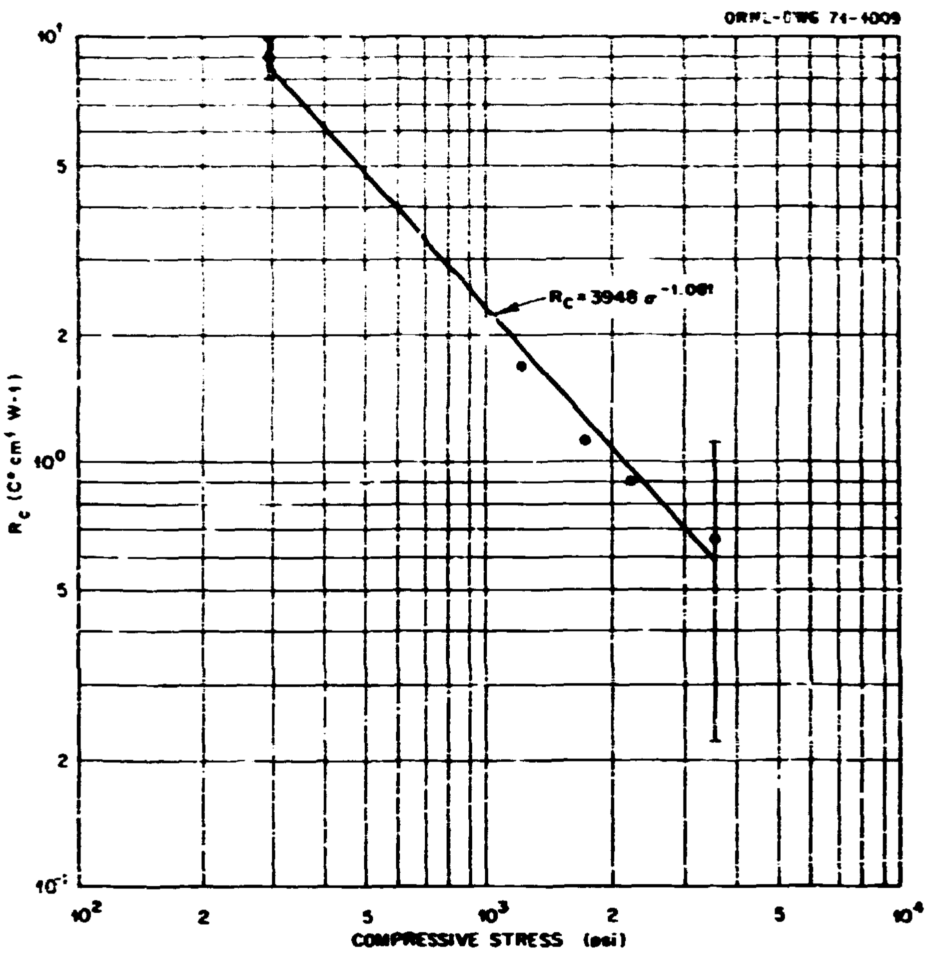

Fig. 18. Thermal Contact Resistance Data (50°C) for Interface Between UN and Molybdenum.

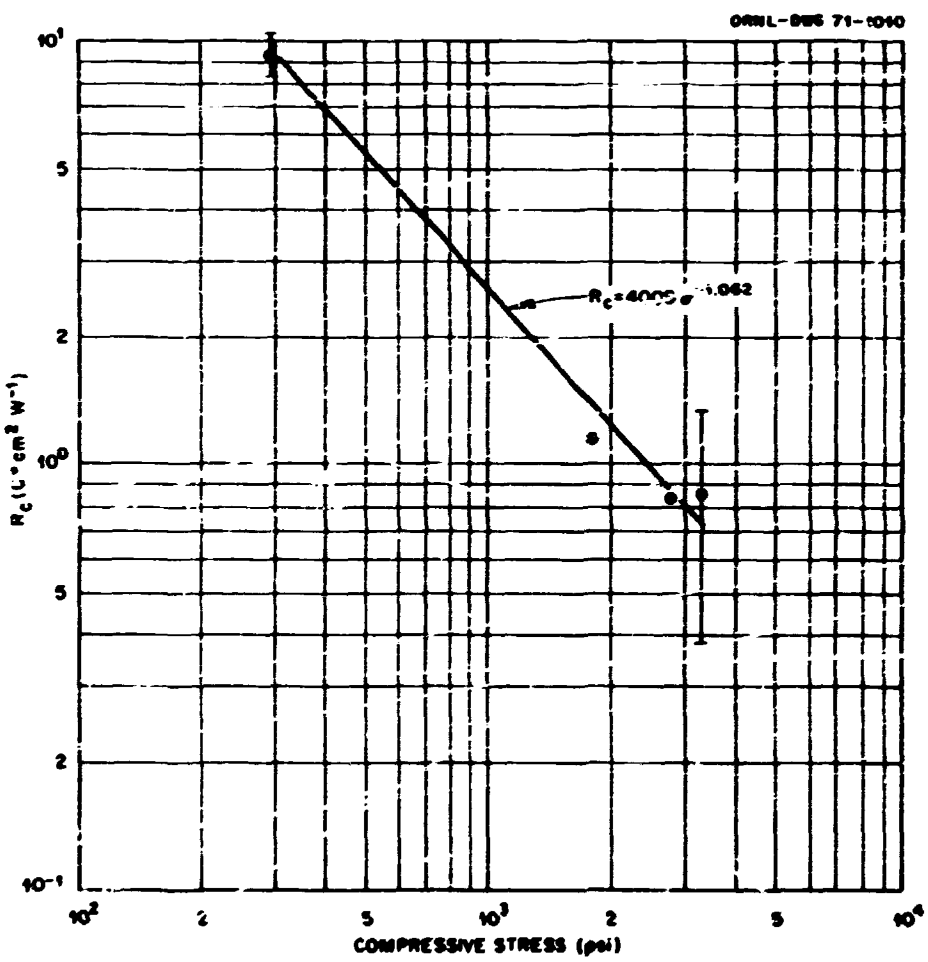

Fig. 19. Thermal Contact Resistance Data (50°C) for Interface Between UN and Half-Hard Type 302 Stainless Steel.

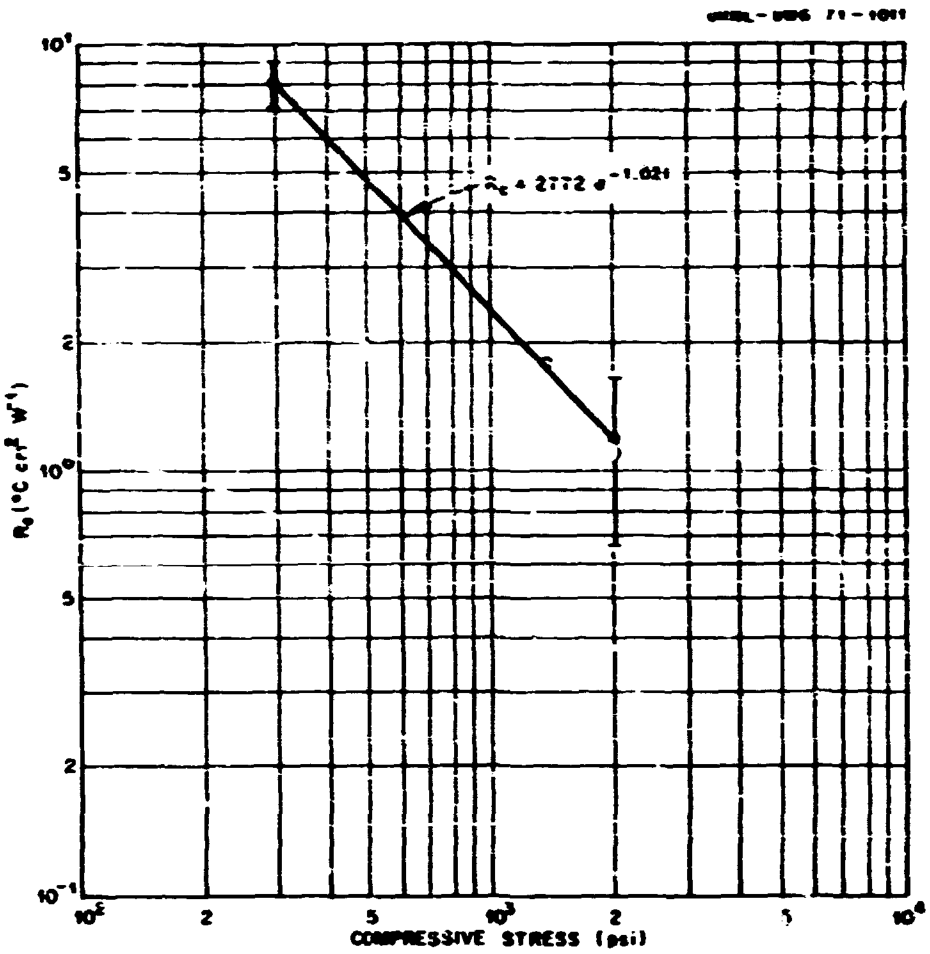

Fig. 20. Thermal Contact Resistance Data (50°C) for Interface Between UN and Full-Hard Type 302 Stainless Steel.

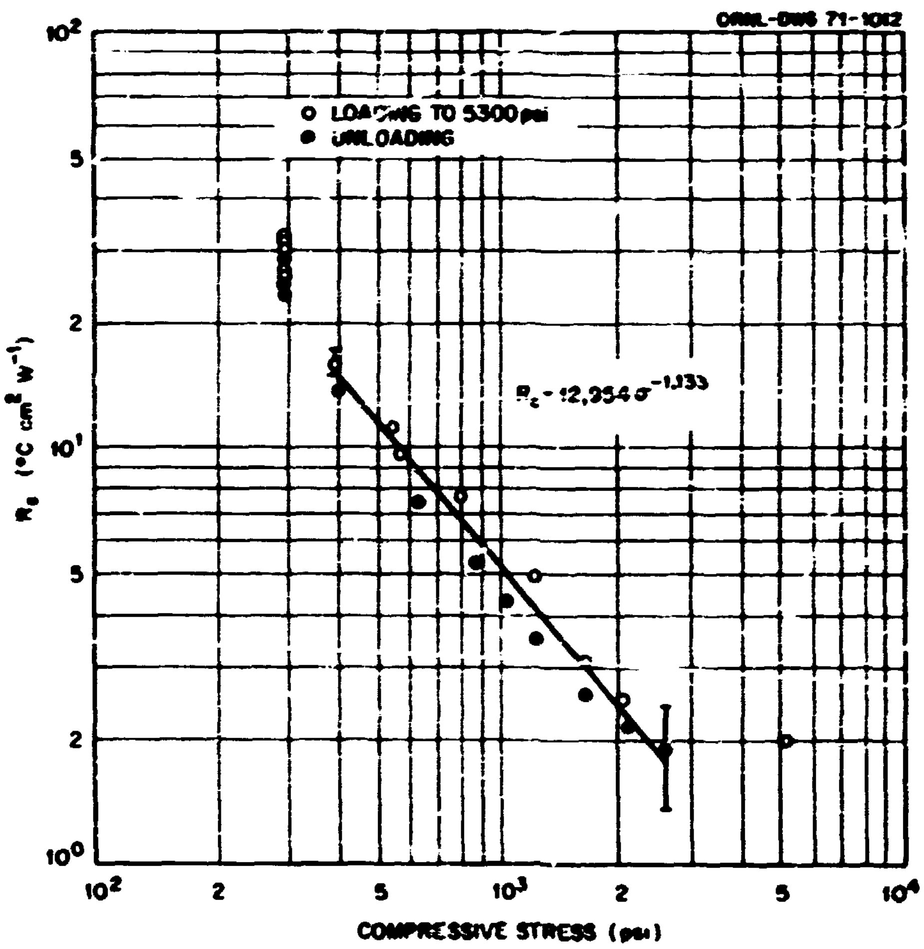

Fig. 21. Thermal Contact Resistance Data (50°C) for Interface Between UN and UN.

DISCUSSION

The principal goal of this study was to determine the relative importance of several variables that probably affect the thermal contact resistance of UN-metal interfaces. As previously mentioned, these variables include stress, surface deformation characteristics, surface topography, and thermal conductivity. Minges[12] gave a clear description of how these parameters enter the picture. A single solid-solid contact is the basic unit of heat transfer for an interface, and the resistance to heat transfer across this unit, r_c, can be written as

$$r_c = \frac{1}{2\lambda a} , \qquad (3)$$

where

a = contact radius, cm, and

λ = the thermal conductivity of the solid.

For the case of contacts between dissimilar materials, λ is usually replaced by the harmonic mean conductivity, λ_m:

$$\lambda_m^{-1} = \frac{1}{N} \sum_i \lambda_i^{-1} , \qquad (4)$$

where N is the number of materials. This procedure is equivalent to computing the average thermal resistivity of a contact and thus assumes that the individual contacts are composed of equal amounts of the two materials. This assumption would not be justified if one of the two surfaces was quite rough while the other was very smooth.

To illustrate the effects of the variables, consider a simplified hypothetical interface with n uniform contacts per unit area. The thermal resistance per unit area, A_a, is R_c, and the heat flow is through n contact resistances acting in parallel:

$$R_c^{-1} = \sum_{i=1}^{n} r_c^{-1} = 2n\lambda_m a . \qquad (5)$$

---

[12]M. L. Minges, Thermal Contact Resistance: A Review of the Literature, vol 1, AFML-TR-65-375 (April 1966).

The actual contact area, A_c, is a fraction, ξ, of the geometrical contact area, A_a (1 cm^2):

$$A_c/A_a = \xi \ . \tag{6}$$

Also,

$$\xi = n\pi a^2 \ , \tag{7}$$

and

$$R_c = \frac{\sqrt{\pi}}{2(\xi n)^{1/2}\ \lambda_m} \ . \tag{7}$$

Equation (7) illustrates the fact that R_c depends on both the actual contact area, ξ, and the number of contact spots per unit area, n. All other variables except corrosion films enter the problem because they change n and ξ.

Application of a stress can increase the size of existing contacts and can create new ones; the deformation characteristics of the surface determine how effective a given stress level will be in creating and enlarging surface contacts. Surface topography controls the initial number and size of the contact spots and also influences the number of new contacts formed when a larger stress is applied. Thus, the problem of determining R_c is very complicated, and there is a strong likelihood that the variables will interact. Also, since the interfaces examined in this study represent a wide range of conditions, it seems unlikely that a simple, semiempirical correlation would describe all of the effects. There is no single, general correlation to which all of the data can be compared, but published work does provide a useful guide for determining the probable effects of the variables. Therefore, it seems logical first to examine some of the individual variables.

Stress

Compressive stress, σ, has a strong influence on thermal contact resistance. Consideration of single solid-solid contacts leads to the predictions[12]

$$R_c \propto 1/\sigma^{1/3} \text{ (elastic compression)}$$

$$R_c \propto 1/\sigma^{1/2} \text{ (plastic compression) .}$$

As shown in Figs. 13 to 21, fitting the R_c values to the equation

$$R_c = A/\sigma^\delta \tag{8}$$

produces exponents of 0.83 to 1.38. This type of behavior is usually explained by assuming that the number of contact spots per unit area increases with increasing load (i.e., that new contact spots are created as the stress increases and the old spots enlarge). Obtaining a larger stress exponent would also suggest that most of the deformation would be plastic. If this were true, the R_c values should depend on the hardness or tensile strength of the softer material rather than on elastic moduli. The differences between exponents, δ, obtained for various interfaces are probably not significant because the data for R_c at high stress were not very accurate, and the stress range for the data seemed to influence the value of the exponent (Figs. 16 and 19). Thus, representation of the R_c data by Eq. (8) must be viewed as only a convenient method for smoothing data for a limited range of stress. A corollary of this observation is that use of a single exponent to describe the stress dependence for all the interfaces would probably be justified.

Time at Stress

For some of the softer materials, the R_c curves shifted after prolonged application of high stresses, probably because of the deformation characteristics of the surface material. This behavior is illustrated by the 12% decrease in 10 days found for indium (Appendix A) and the major hysteresis noted with copper and 1100 aluminum foils. The data for the UN-Cu interface (Fig. 15) show that prolonged application of 5350-psi stress reduced R_c by about a factor of 2 and also seemed to alter the dependence on stress. These changes are presumably due to creep at the solid-solid contacts, which would tend to increase the size of the individual contacts. Further reductions in R_c might, therefore, be expected if the creep rate were increased through increases in temperature or stress level.

The data for 1100 aluminum (Fig. 14) show a similar effect. In this case, loading and unloading did not change the curve for R_c versus σ, but R_c increased when the foil was moved relative to the two UN specimens. This increase in R_c was then removed and the original curve for R_c versus σ was reestablished when the sample was held at a stress of 5700 psi for 23 days. Data for surface roughness and metallographic examination of the 1100 aluminum (Table 1 and Figs. 4 and 5) surface indicate that a considerable amount of plastic flow took place during the tests; the sample appeared smoother after the tests. The observations for 1100 aluminum are rationalized as follows:

1. The creep rate of 1100 aluminum was higher than that of copper; this permitted more rapid plastic deformation at the solid-solid contacts. The initial 300-psi load may even have caused a considerable amount of plastic flow. Under these conditions the loading and unloading curves would be expected to superimpose.

2. When the samples were moved, the asperities on the UN samples were indenting cold-worked material, and the surface match created by the first load cycle was lost. This increased R_c (decreased the area of solid-solid contact), but the increase was removed by further plastic deformation at 5700 psi.

3. The fact that the data obtained after the stress cycle fell on the original curve for R_c versus σ suggests that the surface characteristics of the UN controlled the contact area.

The data for the interface between UN and In also seem to show some time dependence, and, furthermore, the R_c values were considerably higher than expected. The latter point is illustrated by comparing the value for R_c at 300 psi, 3.2 deg cm^2 W^{-1}, with values obtained by Moore et al.[13] for interfaces between Fe and In, 0.06 deg cm^2 W^{-1}, and the value quoted

[13]J. P. Moore, T. G. Kollie, R. S. Graves, and D. L. McElroy, Thermal Conductivity Measurements on Solids Between 20 and 150°C Using a Comparative-Longitudinal Apparatus: Results on MgO, BeO, ThO_2, $Th_xU_{1-x}O_{2+y}$ and Al-UO_2 Cermets, ORNL-4121 (June 1967).

by Bauerle et al.[14] for indium soldered surfaces, 0.05 deg cm^2 W^{-1}. If the R_c value for soldered surfaces is taken to represent "complete" solid-solid contact, then extrapolation of the data would indicate that a stress of about 16,000 psi would be required for total solid-solid contact at the UN-In interface studied. The relatively high R_c value obtained for the UN-In interface also makes it difficult to apply the data to some existing, semiempirical R_c correlations.[15] These correlations generally predict that R_c is a product of several factors, one of which should approach zero as the material becomes very soft. The lack of agreement with the data of Moore et al.[13] is not a serious problem, since their Armco iron surfaces were much smoother than the surfaces of the UN specimens and since the difference in λ between Armco iron and UN also favors a lower value for R_c [Eq. (7)]. Also, the errors are large for both sets of data, and the stress levels determined by Moore et al.[13] were considerably more uncertain than the present values.

A time dependence for the area of individual solid-solid contacts does not offer a reasonable explanation of the high R_c values. For indium, 50°C is a very high temperature, and plastic flow is quite rapid. Both the hardness and tensile strength (380 psi) (ref. 16) of indium are only about 3% of the values for 1100 aluminum. With this situation, the plastic flow obtained after an increase in stress should take place long before the thermal steady state is reestablished (10 to 12 hr), and no time dependence should be noted. Also, since the compressive stresses employed were greater than the ultimate tensile stress, full plastic flow should be initiated for all stresses. Unfortunately, since the run was catastrophically terminated before R_c values for the

---

[14] J. E. Bauerle, P. H. Sutter, and R. W. Ure, Jr., "Measurements of Properties of Thermoelectric Materials," p. 285 in Thermoelectricity: Science and Engineering, ed. by R. R. Heikes and R. W. Ure, Jr., Interscience, New York and London (1961).

[15] C. L. Tien, "A Correlation for Thermal Contact Conductance of Nominally-Flat Surfaces in Vacuum," pp. 755–759 in Thermal Conductivity, Proc. 7th Conf., Nat. Bur. Std. Tech. Publ. 302, ed. by D. R. Flynn and B. A. Peavy, Jr., National Bureau of Standards, Washington, D. C., September 1968.

[16] Metals Handbook, 8th Edition, 1961, p. 120.

unloading cycle could be obtained, we do not know if hysteresis would have been obtained. However, if we judge on the basis of the behavior of 1100 aluminum, this does not seem to be a likely possibility.

The most likely explanation of the high R_c values for the UN-In interface is that something prevented plastic flow of the indium into the valleys between asperities. This could have been caused by trapped air or possibly a reaction between UN and indium. Indium forms a good vacuum seal, and assembly of the test column was carried out in air and involved application of stresses of about 1000 psi; air might have been trapped in the crater-like (Fig. 2) surfaces of the UN. Also, the high self-diffusion coefficient of indium might have promoted formation of an amalgam-like product with UN. However, cursory examination of the indium foil after the test did not reveal any obvious reaction product. Long-range plastic flow and extrusion of indium out of the interface probably gave rise to the small time dependence. This process would have the effect of moving the indium parallel to the UN surfaces and thus might be expected to have created some additional area of solid-solid contact by a smearing action.

Time also seemed to have an influence on R_c values for the least plastic, highest R_c interface studied, that between UN and UN. Data obtained during the first 10 days of the run show $R_c^{50°C}$ decreased 20% at 300 psi. The column was then unloaded to replace the bottom lead foil with indium, and the two specimens were reassembled. After this alteration, the R_c of the interface at 300 psi returned to the original value. This variation was presumably due to thermal cycling, since the largest change took place when the temperature of the interface was altered. Presumably, differential thermal expansion or vibration could have permitted the two mating surfaces to move slightly and to provide a greater area of contact.

The hysteresis effects noted above clearly show that time at stress and/or the maximum stress level would have to be included in a general correlation that would describe all of the data that have been presented. In principle, this could be accomplished by including a mathematical description of the time-dependent deformation of surface asperities, but the problem appears to be quite formidable. A simpler alternative is to examine the behavior of the more-or-less stable R_c values obtained after high stresses had been applied. A correlation based on these data should still show the effects of short-time deformation (hardness) and thermal conductivity of the mating surfaces. However, the available surface data (Table 1) are probably rather weak, since profilometer rms roughness values do not give a full surface characterization.[17] Also, since the variables are expected to interact,[18] discussion of the effects of single parameters cannot be continued; a more general approach is indicated.

Correlation Via Tien's Method

C. L. Tien[15] (see Appendix B) proposed a semiempirical correlation for nominally flat, random surfaces in vacuum that might apply to data obtained in this study. The correlation, which employs three dimensionless groups, can be stated as

$$\frac{\gamma}{R_c \lambda_m} = b m^g \left(\frac{\sigma}{H}\right)^d \qquad (9)$$

where

γ = rms surface roughness,
$= \sqrt{\gamma_1^2 + \gamma_2^2}$ for random surfaces (ref. 15),
b, g, d = constants,
m = rms slope (ref. 15), and
H = hardness.

The parameter m is included to account for the effect of contact density [Eq. (7)] on R_c. Tien[15] showed that this correlation worked reasonably

[17] H. E. Bennett and J. O. Portens, J. Opt. Soc. Am. 51, 123 (1961).

[18] M. L. Minges, Thermal Contact Resistance: A Review of the Literature, vol 1, AFML-TR-65-375 (April 1966).

well for $10^{-5} < \gamma/R_c\lambda_m < 3 \times 10^{-3}$ and $10^{-4} < \frac{\sigma}{H} < 3 \times 10^{-2}$ and proposed for the constants

$b = 0.55$,

$g = 1.0$, and

$d = 0.85$.

Although the assumption of a random surface is suspect, data from this study can be used to test the hypothesis

$$\frac{\gamma}{R_c\lambda_m} \propto \left(\frac{\sigma}{H}\right)^d .$$

The appropriate plot is shown in Fig. 22, but values for the interface between UN and In were omitted because a reliable value for the surface parameter γ_1 could not be obtained for indium. The correlation is roughly equivalent to that shown in Tien's Figs. 1 and 2 (ref. 19),

[19] C. L. Tien, "A Correlation for Thermal Contact Conductance of Nominally-Flat Surfaces in Vacuum" pp. 755–759 in Thermal Conductivity, Proc. 7th Conf., Nat. Bur. Std. Tech. Publ. 302, ed. by D. R. Flynn and B. A. Peavy, Jr., National Bureau of Standards, Washington, D. C., September 1968.

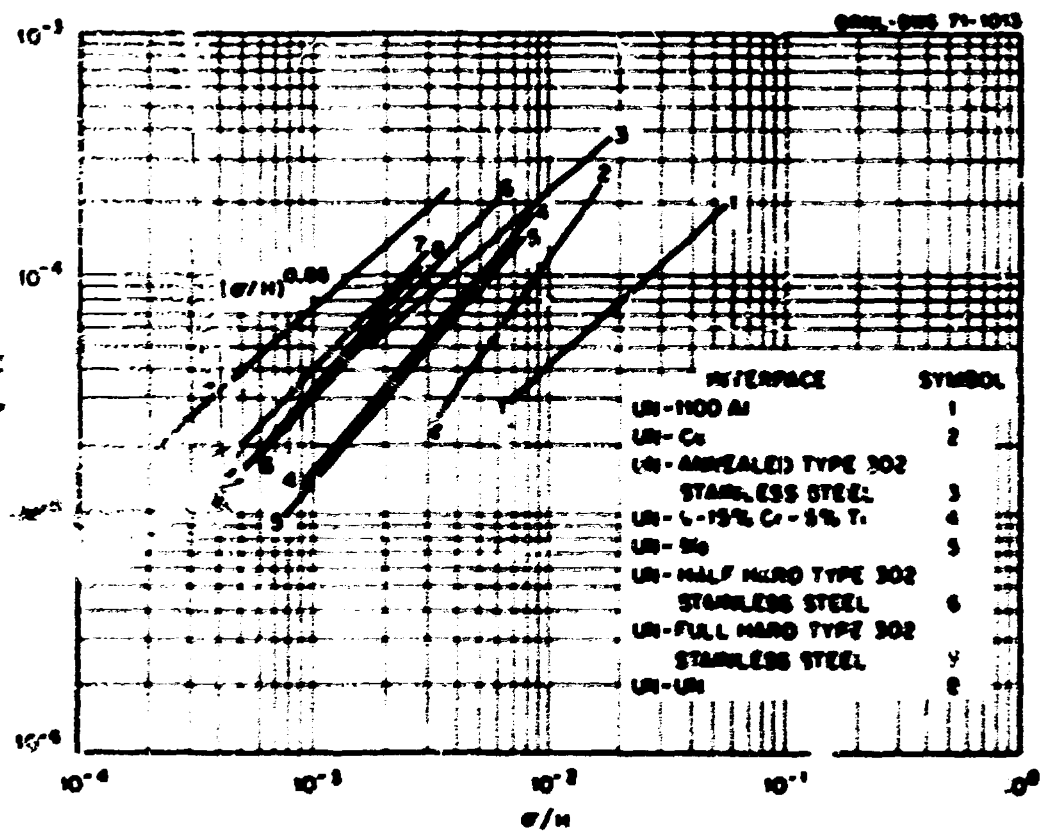

Fig. 22. Tien's Correlation Applied to Data for Interfaces Between UN and a Metal.

and the dimensionless variables calculated for data from our study lie in the same range as the results considered by Tien.

This correlation is really not very satisfying or useful, for it produces a family of roughly parallel lines, and the offsets must be explained by invoking an unmeasured quantity, m, the rms slope. Furthermore, if the average ridge densities are combined with the data for surface roughness (Table 1) to yield relative values of the rms slope, m, for the foils, Table 3 shows that the m values do not correlate with the offsets shown in Fig. 22.

Table 3. Offsets of Curves Shown in Fig. 22[a]

Interface	σ/H at $\gamma/R_c\lambda_m = 5 \times 10^{-5}$	m_{foil}[b]
	$\times 10^{-3}$	$\times 10^{-2}$
UN–type 302 stainless steel (full hard)	1.23	1.09
UN–UN	1.44	
UN–type 302 stainless steel (half hard)	1.56	1.77
UN–type 302 stainless steel (annealed)	1.70	2.88
UN–V–15% Cr–5% Ti	2.80	0.93[1]
UN–Mo	3.12	0.90[3]
UN–Cu	5.40	
UN–1100 Al	12.3	1.39

[a]Tien's correlation (ref. C. L. Tien, "A Correlation for Thermal Contact Conductance of Nominally-Flat Surfaces in Vacuum," pp. 755–759 in Thermal Conductivity, Proc. 7th Conf., Nat. Bur. Std. Tech. Publ. 302, ed. by D. R. Flynn and B. A. Peavy, Jr., National Bureau of Standards, Washington, D.C., September 1968.)

[b]Relative m values for the foils were computed from the relationship

$$m = \gamma D ,$$

where

γ = rms surface roughness, cm, and

D = relative density of ridges (Table 1), lines/cm.

Further examination of Fig. 22 and Table 3 suggests that the offsets are related to the hardness of the interface materials. Since this trend also holds for 11 of the 12 sets of data used by Tien[19] (Figs. 1 and 2 of Appendix B), further examination of the variation is warranted. Rearranging Tien's correlation equation yields

$$R_c = \frac{\gamma}{b\lambda_m m^{\beta}} \left(\frac{H}{\sigma}\right)^d \quad . \tag{9a}$$

The experimental data from this study can be described by equations of the form

$$R_c = A/\sigma^{\delta} \tag{8}$$

where $0.8 \leq \delta \leq 1.4$. Tien's correlation assumed the exponent d to be common to all interfaces; therefore, a common value for δ must be chosen before proceeding. As previously mentioned, the differences between empirical δ values are not very significant; therefore, for simplicity's sake, we assume $\delta = 1.0$ for all interfaces. A new A value for each foil, A′, [Eq. (8)] can then be calculated, and the variation in A′ should be consistent with Tien's correlation. Since the most accurate R_c data are the values for low stresses, we computed the A′ values for the lowest stresses available for each run. Substitution of Eq. (8), with $\delta = 1$, into Eq. (9a) yields

$$A' = \frac{\gamma}{b\lambda_m m^{\beta}} (H) \quad , \tag{10}$$

and, since λ_m and γ values are available for most foils, we would expect

$$\frac{A'\lambda_m}{\gamma} \approx \frac{1}{b m^{\beta}} (H) \quad .$$

The most important feature shown in the hardness plot in Fig. 23 is that the data roughly follow the equation

$$\frac{A'\lambda_m}{\gamma} = \alpha + \beta H \quad . \tag{11}$$

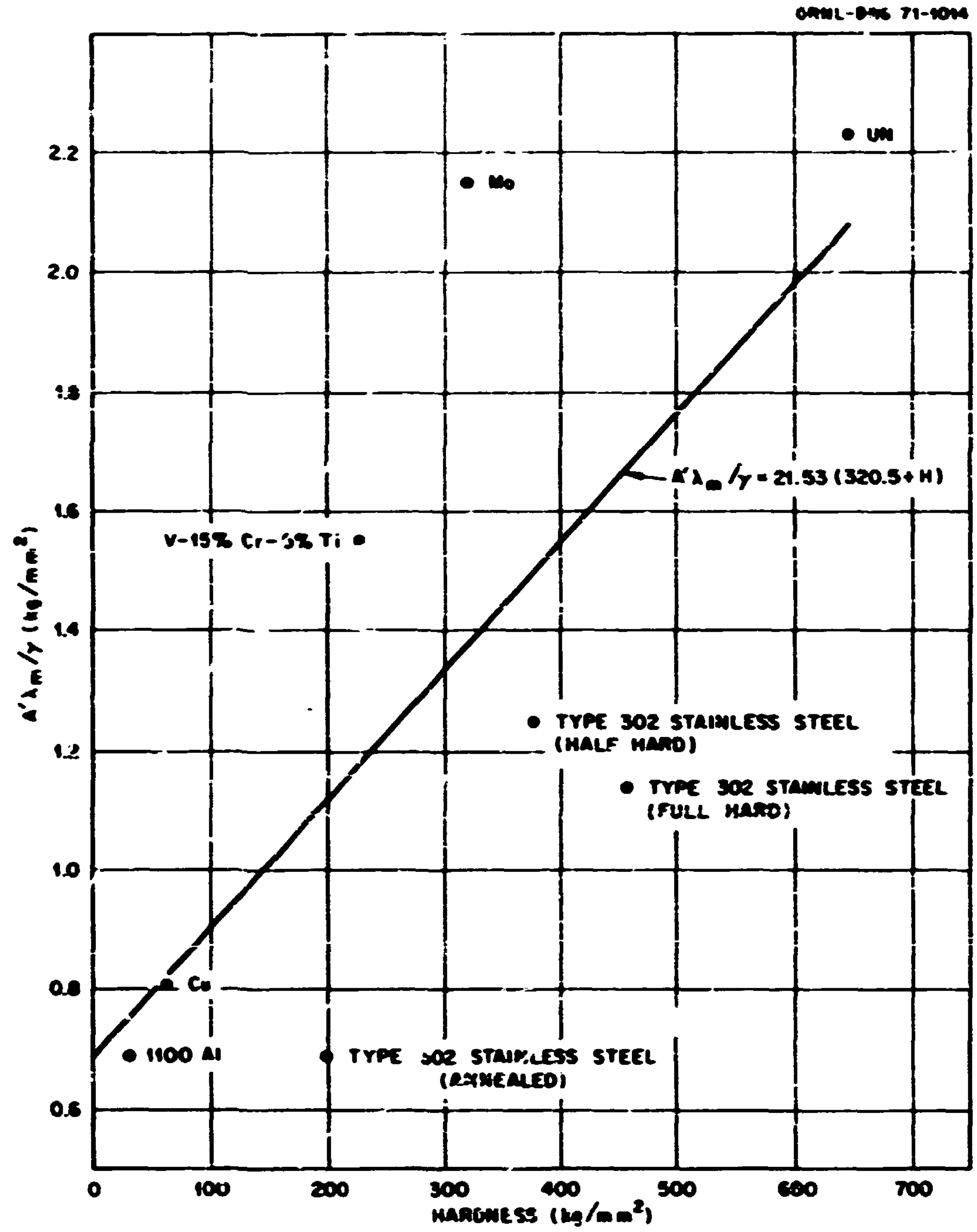

Fig. 23. Effect of Foil Hardness (VHN) on the Parameter $\frac{A'\lambda_m}{\gamma}$.

The presence of an intercept was also consistent with the results for the UN-In interface, which indicated that R_c did not approach zero for a very soft foil.

Individual points are scattered about the line for the least-squares fit,

$$\frac{A'\lambda_m}{\gamma} = 21.53\ (320.5 + H) \quad , \tag{11a}$$

by as much as +55%, but Eq. (9a) indicates that this difficulty might be due to neglecting the rms slope factor, m. The relative m values for the foils shown in Table 3 can be used to test this hypothesis. Expressing the deviations for individual points in terms of a multiplication factor, f(m),

$$\frac{A'\lambda_m}{\gamma} = f(m)\ (\alpha + \beta H) \quad , \tag{11b}$$

we would expect

$$f \propto m^{-g}$$

where g ≅ 1.0 (Tien). Figure 24 shows that for five of the six interfaces

$$f = 4.107 \times 10^{-2}\ m^{-0.750} \quad . \tag{12}$$

This observation indicates that the density of contact points is an important parameter for UN-metal interfaces, and the exponent g is reasonably close to Tien's estimate.

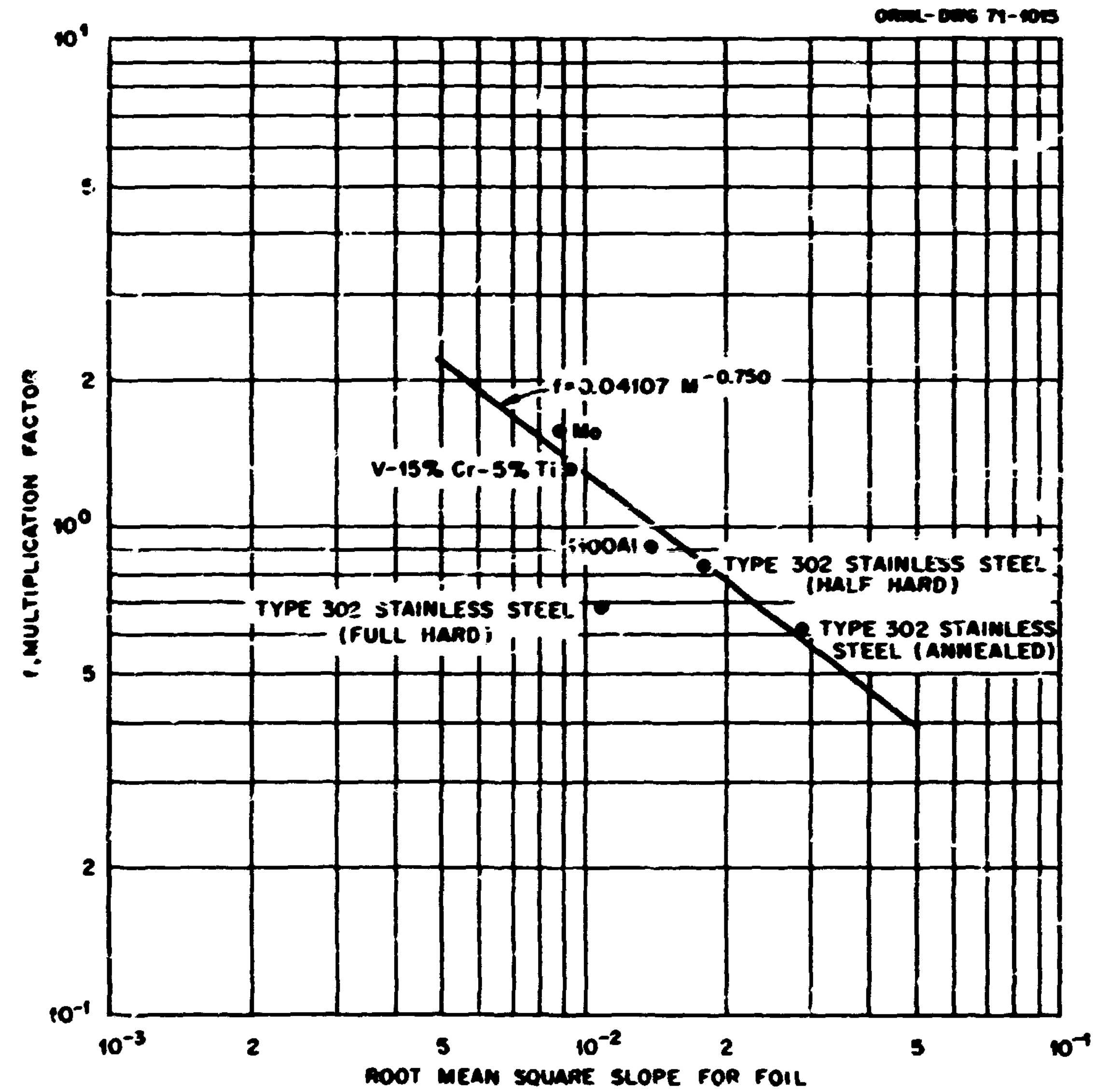

Fig. 24. Multiplication Factor (f) Versus Relative Root-Mean-Square Slope Value (m) for Metal Foils.

Data for the sixth interface, that between UN and full-hard type 302 stainless steel, do not follow this trend. This anomaly might possibly be related to additional contact area caused by elastic deformation. This work-hardened foil was also very smooth (Table 1), and, under these conditions, plastic flow might not have been responsible for all of the contact area.

However, a modified form of Tien's correlation gives a reasonable description of most of the data:

$$R_c = \frac{0.884\ \gamma(320.5 + H)}{\lambda_m m^{0.75}\ \sigma}\ , \tag{13}$$

where σ is in kg/mm^2. The value of b (0.884^{-1}) [Eq. (9)] is just over a factor of 2 larger than the b obtained by Tien (0.55), but inclusion of a second constant [α in Eq. (11)] tends to offset this difference. The two correlation equations would thus be in good numerical agreement for hardness values around 300 kg/mm^2, and this agreement means that the R_c data for UN-metal interfaces are also roughly consistent with the results of the experimental studies used by Tien.

Deviations of the smoothed R_c data from Eq. (13) are shown in Fig. 25. Relative rms slope values were not available for the interfaces of UN with indium, copper, and UN, but data from these runs are also roughly consistent with Eq. (13). Values of $\gamma/m^{0.75}$ for the three interfaces were calculated from Eq. (13) and found to lie within the range of $\gamma/m^{0.75}$ for the other six interfaces.

Once a correlation that describes most of the R_c data has been obtained, it is instructive to consider how much the various factors affect the R_c of UN interfaces. If we choose the interface of UN with UN as a basis for comparison, we see that material variations could change the λ_m and H factors. Maximum improvement ratios from these sources would be

$$\lambda_m : \frac{0.265}{0.137} = 1.93$$

for copper and UN and

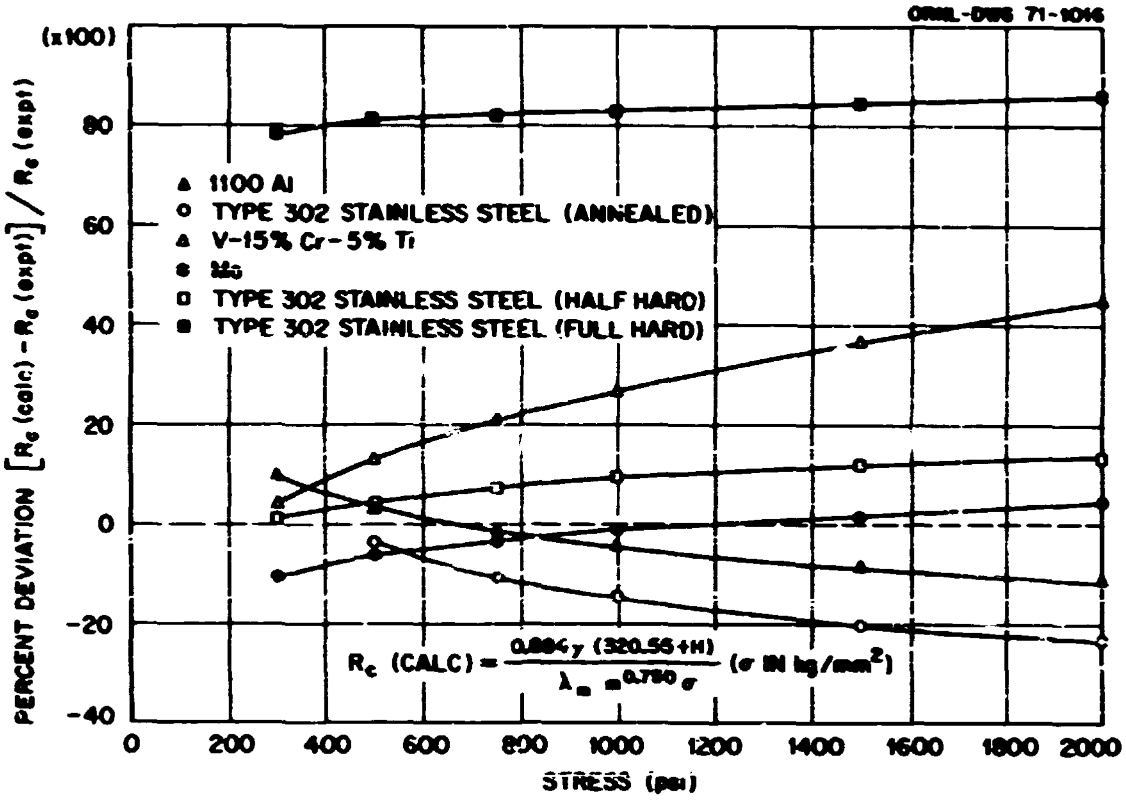

Fig. 25. Deviations of Smoothed [Eq. (8)] R_c Values from Modified Tien Correlation [Eq. (13)].

$$H : \frac{320.5 + 649}{320.5} = 3.02$$

for indium and UN, for a maximum hypothetical materials factor of 5.8. The surface factor is more complicated. Data for the interface of UN with UN indicate $\gamma/m^{0.75} \cong 6.55 \times 10^{-4}$. Two mating surfaces with $\gamma = 1.27 \times 10^{-6}$ cm and $m = 0.1$ (ref. 20) would produce $\gamma/m^{0.75} = 1.0 \times 10^{-5}$ or an improvement by a factor of 65. Surface modifications thus appear to offer a more promising method for reducing R_c, but routine production of high-quality mating surfaces would not be cheap or easy.

CONCLUSIONS AND RECOMMENDATIONS FOR FUTURE WORK

Analysis of the experiments performed in this study leads to the following conclusions.

---

[20] C. L. Tien, "A Correlation for Thermal Contact Conductance of Nominally-Flat Surfaces in Vacuum," pp. 755–759 in Thermal Conductivity, Proc. 7th Conf., Nat. Bur. Std. Tech. Publ. 302, ed. by D. R. Flynn and B. A. Peavy, Jr., National Bureau of Standards, Washington, D. C., September 1968.

1. Thermal contact resistance decreases as the compressive stress at an interface is increased. Over limited stress ranges, the decrease can usually be described by an empirical equation:

$$R_c = A/\sigma^{\delta}$$

where $\delta \cong 1.0$. Data obtained over a larger range of compressive stress would be useful for testing this equation, since the results of this study suggest that the exponent δ decreases at high stresses.

2. At the temperature levels used in this study, R_c decreases slowly with increasing temperature. Further investigation of the temperature dependence is needed, and it would be particularly interesting to obtain R_c data at the knee of curves for hot hardness versus temperature. Such an experiment could most readily be carried out by choosing a foil material that softened rapidly near room temperature. Tin, lead, and their alloys are likely candidates for this study.

3. Hysteresis was found to be significant for the 1100 aluminum and copper foils; the R_c values decreased with time at stress and maximum stress level. A more quantitative understanding of these changes is greatly needed if successful R_c predictions are required.

4. Other factors that affect R_c seem to be roughly consistent with Tien's correlation, but a broader range of experiments would be useful in determining the range of validity of this correlation. In particular:

(a) The observation that R_c did not approach zero for the softest foils should be investigated further. Factors that prevent complete solid-solid contact are obviously important for practical applications, and identification of those factors might lead to significant improvements in the performance of fuel elements.

(b) Thermal conductivity does not appear to be a very critical parameter, but this observation should be checked by additional experiments on low λ_m interfaces such as those between UN and Teflon or UN and glass. The validity of the λ_m average should also be investigated, since λ_m may not apply when surfaces with significantly different rms roughnesses are involved.

(c) Surface characteristics seem to play an important role and should be investigated on a more quantitative basis. In particular, the large improvements in R_c values suggested for high rms slope (m) surfaces should be checked experimentally, and, if these are confirmed, practical methods for producing high m surfaces should be developed.

APPENDIX A

Table A-1. Thermal Contact Resistance Data for Interface of UN and Indium

Time[a] (days)	Temperature (°C)	R_c^0/R_c^{90} [b]	$\bar{R}_c$ (deg cm^2 W^{-1})	$\bar{R}_c^{90°C}$ (deg cm^2 W^{-1})	Compressive Stress (psi)	Remarks
1	34.52	1.16	3.04	2.76	296	
3	44.00	1.08	3.70	3.56	296	Realigned column; loaded to 1000 psi before taking data.
5	60.24	1.07	2.98	3.20	296	
6	43.92	1.09	3.33	3.20	296	
7	47.71	1.02	1.98	1.95	436	
17	47.78	1.00	1.72	1.70	429	12.8% decrease in 10 days. Normalized last 3 points by this amount.
19	49.27	0.98	1.40	1.39	576	
21	52.72	0.82	0.659	0.671	1181	

[a] From beginning of run when load first applied.

[b] Ratio of two independent R_c values.

Table A-2. Thermal Contact Resistance Data for Interface of UN and 1100 Aluminum

Time (days)	Temperature (°C)	R_c^0/R_c^{90}	$\bar{R}_c$ (deg cm^2 W^{-1})	$\bar{R}_c^{90°C}$ (deg cm^2 W^{-1})	Compressive Stress (psi)	Remarks
1	42.25	1.20	3.92	3.87	296	No high stresses prior to this measurement.
7	53.73	0.96	1.60	1.64	462	
8	50.59	0.84	1.41	1.42	544	
9–24						Stress raised to 7100 psi and released.
25	58.89	1.01	0.421	0.448	2335	
28	57.83	1.10	0.559	0.590	1645	
29–41						Stress raised to 6200 psi and released; specimen moved slightly after all load removed.
42	48.57	1.01	5.02	4.97	296	
49	51.23	0.99	3.20	3.23	462	
50	53.93	0.97	2.64	2.71	735	
52	57.73	0.84	1.69	1.78	1335	
53–76						Stress raised to 5700 psi and released.
77	58.38	1.03	0.739	0.783	1489	
78	57.53	1.15	0.960	1.011	1100	
91	51.40	1.12	2.65	2.68	296	
92	61.95	1.19	2.27	2.46	296	
94	34.16	1.06	2.10	1.90	296	

BLANK PAGE

Table A-3. Thermal Contact Resistance Data for Interface of UN and Copper

Time (days)	Temperature (°C)	[illegible]/R°_c	$\bar{R}_c$ (deg cm² W⁻¹)	$\bar{R}_c$ [illegible] °C (deg cm² W⁻¹)	Compressive Stress (psi)	Remarks
1	[illegible]	[illegible]	[illegible]	[illegible]	[illegible]	
2	[illegible]	[illegible]	[illegible]	[illegible]	[illegible]	
3	[illegible]	2.00	[illegible]	3.44	[illegible]	
[illegible]	41.64	1.02	7.62	7.22	[illegible]	
7	[illegible]	[illegible]	[illegible]	[illegible]	[illegible]	
8	41.16	[illegible]	[illegible]	[illegible]	[illegible]	
[illegible]	48.42	[illegible]	[illegible]	[illegible]	[illegible]	
10	[illegible]	[illegible]	[illegible]	[illegible]	417	
14	44.36	1.11	[illegible]	4.68	[illegible]	
14	[illegible]	[illegible]	[illegible]	[illegible]	600	
15	[illegible]	1.13	[illegible]	9.62	296	
16	[illegible]	[illegible]	[illegible]	1.74	721	
25	[illegible]	[illegible]	1.72	1.79	[illegible]	
26–36						Stress raised to 5600 psi and released.
37	[illegible]	[illegible]	[illegible]	[illegible]	1209	
38	[illegible]	[illegible]	1.15	1.36	[illegible]	
39	[illegible]	1.17	4.90	5.08	296	
42	[illegible]	[illegible]	[illegible]	[illegible]	427	
43	[illegible]	[illegible]	1.01	[illegible]	427	
45	[illegible]	[illegible]	0.584	0.613	1267	
46–66						Stress raised to 6600 psi and released.
67	[illegible]	[illegible]	[illegible]	[illegible]	1480	
70	60.27	1.13	[illegible]	[illegible]	1024	
73	59.28	1.18	0.660	0.703	850	
74	58.87	1.17	0.815	0.866	[illegible]	
77	[illegible]	1.19	0.927	0.927	720	
79	53.04	1.20	1.34	1.37	548	
85	51.15	1.20	2.78	2.80	333	
86	50.36	1.19	3.20	3.21	296	
87	61.41	1.20	3.21	3.47	296	
88	60.98	1.18	3.44	3.73	296	
91	36.51	1.14	2.73	2.47	[illegible]	
92	48.10	1.17	3.30	3.26	296	

Table A-4. Thermal Contact Resistance Data for Interface of UN and Annealed Type 302 Stainless Steel

Time (days)	Temperature (°C)	R_c'/R_c''	$\bar{R}_c$ (deg cm² W⁻¹)	$\bar{R}_c$ [illegible]°C (deg cm² W⁻¹)	Compressive Stress (psi)	Remarks
[illegible]	[illegible]	[illegible]	[illegible]	[illegible]	[illegible]	
1[illegible]	[illegible]	[illegible]	[illegible]	[illegible]	[illegible]	
14	[illegible]	[illegible]	[illegible]	[illegible]	1[illegible]	
1[illegible]	[illegible]	[illegible]	1.[illegible]	[illegible]	[illegible]	
1[illegible]	[illegible]	[illegible]	[illegible]	4.[illegible]	[illegible]	
[illegible]	[illegible]	[illegible]	[illegible]	[illegible]	[illegible]	
[illegible]	[illegible]	[illegible]	[illegible]	[illegible]	[illegible]	
[illegible]	[illegible]	[illegible]	[illegible]	[illegible]	1[illegible]	
[illegible]	[illegible]	[illegible]	1.[illegible]		[illegible]	R_c vs temperature (Fig. 12)
[illegible]	[illegible]	[illegible]	1.[illegible]		11[illegible]	R_c vs temperature (Fig. 12)
[illegible]	12[illegible]	[illegible]	1.1[illegible]		1[illegible]	R_c vs temperature (Fig. 12)
[illegible]	1[illegible]	1.[illegible]	1.[illegible]		[illegible]	R_c vs temperature (Fig. 12)

Table A-5. Thermal Contact Resistance Data for Interface of UN and V-15% Cr-5% Ti Alloy

Time (days)	Temperature (°C)	R_c'/R_c''	$\bar{R}_c$ (deg cm² W⁻¹)	$\bar{R}_c$ [illegible]°C (deg cm² W⁻¹)	Compressive Stress (psi)	Remarks
1	44.48	1.09	11.9[illegible]	11.52	296	
2-[illegible]						Stress raised to 5300 psi and released.
3	48.60	0.84	0.487	0.784	2755	
20	67.14	1.12	1.11	1.2[illegible]	[illegible]	
39	52.20	1.20	10.99	11.16	296	
40	61.87	1.00	1.02	1.11	2027	
41						Stress raised to 4400 psi and released.
42	29.43	1.07	11.77		296	R_c vs temperature (attempt)
43	28.60	1.09	11.06		296	R_c vs temperature (attempt)
43	54.[illegible]	1.21	11.2[illegible]		296	R_c vs temperature (attempt)
44	56.67	1.22	10.20		296	R_c vs temperature (attempt)

Table A-6. Thermal Contact Resistance Data for Interface of UN and Half-Hard Type 302 Stainless Steel

Time (days)	Temperature (°C)	R_c^0/R_c^{50}	$\bar{R}_c$ (deg cm^2 W^{-1})	$\bar{R}_c^{50°C}$ (deg cm^2 W^{-1})	Compressive Stress (psi)	Remarks
1						Stress raised to 5100 psi and released.
2	52.34	0.86	0.828	0.841	2798	
3	72.48	1.14	7.91	9.30	296	
3	52.87	1.03	1.15	1.17	1792	
4	51.28	0.91	0.867	0.874	3291	

Table A-7. Thermal Contact Resistance Data for Interface of UN and Molybdenum

Time (days)	Temperature (°C)	R_c^0/R_c^{50}	$\bar{R}_c$ (deg cm^2 W^{-1})	$\bar{R}_c^{50°C}$ (deg cm^2 W^{-1})	Compressive Stress (psi)	Remarks
1–2						Stress raised to 4600 psi and released.
3	64.66	0.99	0.597	0.603	3540	
9	51.22	1.18	8.94	9.01	296	
10	57.44	1.07	1.61	1.69	1213	
11	58.80	0.89	1.06	1.12	1743	
12	60.49	0.81	0.854	0.920	2234	

Table A-8. Thermal Contact Resistance Data for Interface of UN and Full-Hard Type 302 Stainless Steel

Time (days)	Temperature (°C)	R_c^0/R_c^{50}	$\bar{R}_c$ (deg cm^2 W^{-1})	$\bar{R}_c^{50°C}$ (deg cm^2 W^{-1})	Compressive Stress (psi)	Remarks
1						Stress raised to 5500 psi and released.
2	53.79	1.15	1.15	1.16	1598	
3	54.51	0.92	1.08	1.11	2010	
4	70.40	0.86	6.99	8.09	296	
7	54.78	1.17	1.76	1.81	1359	

Table A-9. Thermal Contact Resistance Data for Interface of UN and UN

Time (days)	Temperature (°C)	R_c^0/R_c^{90}	$\bar{R}_c$ (deg cm^2 W^{-1})	$\bar{R}_c^{50°C}$ (deg cm^2 W^{-1})	Compressive Stress (psi)	Remarks
1	50.62	1.07	31.53	31.66	296	
2	50.99	1.06	31.43	31.63	296	
6	31.99	0.86	34.66	30.94	296	
7	50.02	1.03	26.86	26.86	296	
8	59.98	1.09	25.13	26.92	296	
9	59.99	1.08	24.77	26.52	296	
10	47.85	0.97	26.58	26.20	296	
13	48.29	0.99	25.50	25.21	296	
14	49.16	0.90	16.20	16.11	390	
15	50.61	0.86	11.23	11.28	543	
16	50.36	0.86	11.32	11.34	534	
						Realigned test column; reseated specimens.
1	45.33	1.11	32.57	31.59	296	
2	47.20	1.10	32.90	32.29	296	
6	51.91	0.86	9.73	9.84	565	
7	53.58	0.89	7.59	7.77	800	
8	55.56	0.85	4.76	4.94	1217	
9	57.91	0.87	2.94	3.10	1618	
12	58.85	0.83	2.36	2.51	2036	
13–22						Stress raised to 5300 psi
23	64.08	0.91	1.82	2.01	5192	
24–29						Stress lowered to 2300 psi
30	59.34	0.84	1.78	1.90	2602	
33	58.64	0.88	2.04	2.17	2128	
34	57.57	0.95	2.44	2.57	1642	
36	56.49	1.01	3.31	3.46	1243	
37	55.06	1.09	4.15	4.29	1052	
38	53.62	1.15	5.17	5.30	867	
41	51.76	1.20	7.46	7.55	626	
42	50.50	1.10	13.84	13.88	402	
43	48.28	1.16	29.09	28.76	296	
44	62.16	1.18	21.85	23.77	296	
48	48.90	1.12	25.23	25.05	296	
49	47.77	1.00	27.95	27.54	296	

APPENDIX B

A Correlation for Thermal Contact Conductance of Nominally-Flat Surfaces in a Vacuum

C. L. Tien[1]

University of California
Berkeley, California 94720

A semi-empirical correlation for the thermal conductance of nominally-flat surfaces in a vacuum has been proposed in terms of three dimensionless groups, which characterize, respectively, the thermal contact conductance, the contact pressure, and the surface irregularities. The proposed correlation is shown to be supported quantitatively by previous analytical and experimental investigations.

Key Words: Thermal contact conductance, thermal contact resistance, thermal conductivity, heat conduction, heat transfer.

1. Introduction

The problem of thermal contact conductance has received considerable attention in recent years. Comprehensive surveys of literature on the subject can be found in references [1,2,3,4].[2] In particular, significant progress has been made toward a quantitative analysis of thermal contact conductance in a vacuum environment. Not only is the study of thermal contact conductance in a vacuum of great importance in the thermal design of spacecrafts, but also it serves as a logical starting point for the analysis of the more complex problem involving interstitial fluids. Indeed, impressive analytical groundwork has been laid down by Clausing and Chao [1,5] for macroscopic constriction resistance due to surface waviness or flatness deviations, and by Yovanovich and Fenech [6] and Mikic and Rohsenow [7] for microscopic constriction resistance due to surface roughness of nominally-flat surfaces. Recent analytical attempts also considered the combined effect of surface roughness and waviness upon the overall thermal contact resistance [7,8]. On the other hand, a vast amount of experimental information has become available in recent years. While further analytical and experimental works are needed, the present state of knowledge seems to have reached such a stage that a workable engineering correlation could be constructed for the thermal contact conductance in a vacuum.

The present paper is to establish a correlation for the thermal contact conductance of nominally-flat metallic surfaces in a vacuum environment. Accordingly the effect of surface waviness of flatness deviations is neglected. The correlation, which is based on simple dimensional consideration, consists of three dimensionless groups characterizing respectively the thermal contact conductance, the contact pressure, and the surface irregularities. It is shown that the proposed correlation is in quantitative agreement with previous analytical and experimental results.

2. Dimensional Consideration

Consider two similar metals of nominally-flat, rough surfaces in contact in a vacuum. For dissimilar metals, it is customary to proceed as in the case of similar metals except for the replacement of the metallic physical property by the harmonic mean of those of the dissimilar metals. It is possible, however, to have other complications such as directional effects [9] in the case of dissimilar metals. For this reason, discussions in the present paper will be restricted to the case of similar metals. The rough surfaces under consideration are nominally-flat so that there exists no large-scale waviness

[1]Associate Professor of Mechanical Engineering

[2]Figures in brackets indicate the literature references at the end of this paper.

or flatness deviations. Furthermore, the surface irregularities are assumed to be statistically random and of Gaussian type [10,11]. This is a common assumption for most analyses involving rough surfaces. To describe such a rough surface requires only two statistical parameters, i.e., the rms roughness σ and the autocovariance length a. These two characteristic lengths are related to the rms slope m by the following relation [11]:

$$2\sigma^2 = a^2 m^2 \qquad (1)$$

When two statistically-independent rough surfaces are put in contact, the two characteristic lengths are defined by [7]:

$$\sigma^2 = \sigma_1^2 + \sigma_2^2 \qquad (2)$$

and

$$2(\sigma_1^2 + \sigma_2^2) = a^2(m_1^2 + m_2^2) \qquad (3)$$

It should be noted that, when $\sigma_1 = \sigma_2$ and $m_1 = m_2$, $\sigma = \sqrt{2}\,\sigma_1 = \sqrt{2}\,\sigma_2$ and $m = \sqrt{2}\,m_1 = \sqrt{2}\,m_2$, but still $2\sigma^2 = a^2 m^2$.

To perform a dimensional analysis by use of the Pi theorem [12], it requires first the identification of primary physical parameters in the physical problem. It is natural to have thermal contact conductance h and thermal conductivity λ as two of the primary parameters. The two characteristic lengths σ and a for contact surface irregularities must also be included. In addition, the surface deformation as caused by contact pressure P must be taken into account. For the pressure range of practical interest, it has been shown [6] that the deformation is in the plastic range and the characteristic material property is the microhardness H, which may be conveniently represented by three times the tensile yield stress, i.e., $H = 3F_{ty}$.

From the above consideration, it can be stated that the present problem is characterized by the six parameters, h, λ, σ, a, P and H. Indeed they represent the three major phases of the problem, thermal (h, λ), surface (σ, a), and deformation (P,H). A straightforward application of the Pi theorem leads to the conclusion that there exist three dimensionless groups and they can be logically expressed and related as

$$\left(\frac{h\sigma}{\lambda}\right) = b\left(\frac{\sigma}{a}\right)^{c}\left(\frac{P}{H}\right)^{d} \qquad (4)$$

where the constants b, c, and d are to be determined from theoretical or experimental results. Based on (1), the above equation may be rearranged as

$$\left(\frac{h\sigma}{\lambda}\right) = f m^{g}\left(\frac{P}{H}\right)^{d} \qquad (5)$$

Indeed, an equation of this type has been obtained by Mikic and Rohsenow [7] through their elaborate analysis of the physical problem. Their relation gives $f = 0.9$, $g = 1$, and $d = 16/17$. It should be realized, however, that their analysis is based on idealized physical models. For actual engineering applications, the validity of the relation (4) or (5), and the values of its constants must be determined by the vast amount of experimental data available in the literature.

3. Correlation of Experimental Data

Most existing experimental data do not contain sufficient information to conclusively determine the suggested correlation. In particular, except for the work of MIT group, information concerning a or m is totally missing. Furthermore, all existing measurements of σ and m are of doubtful nature, since they are based on profilometer readings. Bennett and Porteus [11] have not only demonstrated the deficiency in such readings, but also developed an ingenious optical method for the measurements of σ and m. The lack of information on σ and m, however, does not prevent a check on the suggested functional relationship between ($h\sigma/\lambda$) and (P/H). Summarized in Table 1 are experimental investigations with thermal contact conductance data for nominally-flat surfaces in a vacuum. Surfaces are classified here as nominally flat if the rms roughness is greater than one-tenth of the total flatness deviation. Only data for similar metals and for clean surfaces (without plating or oxide films) are included. Actual data points from various investigations are shown in figures 1 and 2 in terms of ($h\sigma/\lambda$) and (P/H).

In view of the wide range of conditions (pressure, temperature, surface and material) under which data were obtained by various investigators, figures 1 and 2 indicate quite convincingly, if not conclusively, that a power relation does exist as

$$\left(\frac{h\sigma}{\lambda}\right) = \left(\frac{P}{H}\right)^{d} \qquad (6)$$

where $d = 0.85$ approximately. The deviations of experimental data from (6) at low values of (P/H) probably result from the waviness effect, which becomes dominant at low contact pressures. The slight

Table 1 Experiments for thermal contact conductance of nominally-flat surfaces in a vacuum (physical properties given in the table are obtained from reference 13)

series	reference	specimen	size D x L (inch)	minimum vacuum (mm-Hg)	flatness deviation (μm)	rms roughness (μm)	rms slope	contact pressure (kN/m^2)	mean contact temp. (°K)	thermal conductivity ($Wm^{-1}deg^{-1}$)	micro-hardness ($10^4 kN/m^2$)
B_A	14	Al 7075-T6	2x1	10^{-5}	15.2	4.67	—	< 7,000	325	0.0083	165
B_S	14	SS 17-4PH	2x1	10^{-5}	10.1	4.07	—	< 7,000	372	0.0015	414
C_A	15	Al 6061-T4	1x1	10^{-5}	1.27	2.59	—	< 700	340	0.0180	33.1
CC_A	5	Al 2024-T4	1/2x2-3/4	10^{-6}	0.38	0.13	—	< 2,200	308	0.0142	104
FA_A	16	Al 6061-T6	2x3	10^{-4}	< 8.9	1.62	—	< 8,300	310	0.0026	725
FA_S	16	SS 304	2x3	10^{-4}	< 2.6	1.56	—	< 8,300	310	0.0015	680
FH_A	17	Al 2024-T4	2x3	10^{-4}	< 8.9	1.63	—	< 8,000	320	0.0121	108
K_S	18	SS 416	1x1-1/2	10^{-6}	(a)	4.30	0.107	< 70,000	430	0.0025	258 (b)
MM_{S1}	7	SS 303	1x1-1/2	10^{-6}	2.03	3.86	0.163	< 8,300	420	0.0017	255 (b)
MM_{S2}	7	SS 303	1x1-1/2	10^{-6}	3.81	4.83	0.150	< 35,000	420	0.0017	255 (b)
MM_{S3}	7	SS 303	1x1-1/2	10^{-6}	3.30	8.64	0.200	< 70,000	430	0.0016	255 (b)
TF_S	6	SS 303	1x1-1/2	10^{-6}	(a)	1.07	0.087	< 28,000	420	0.0017	255 (b)

(a) stated in the reference as nominally flat

(b) value obtained from actual tests indicated in the reference variation of data trend at large values of (P/H) in some series of data (notably, CC_A and FA_A) could be due to a change of deformation characteristic from plastic to elastic range [6].

From their analysis [7], Mikic and Rohsenow have obtained g = 1 in (5). This power dependence on rms slope m is indeed in good agreement with their experimental data. This functional form may also be checked qualitatively from the data presented in figures 1 and 2. Assuming g = 1 and d = 0.85, it follows that all investigations except for CC_A have surfaces with a rms slope m in the range from 0.01 to 0.13, or in terms of angle, from 1/2 to 10 degrees. This seems to agree qualitatively with other surface characterization studies [19]. The value of m for CC_A data is extremely small (m = 0.0001), and this could be caused by an error in their estimate of σ.

With given values of g and d, the correlation can now be established from the experimental information. It is thus proposed the following correlation for the thermal contact conductance of nominally-flat metallic surface in a vacuum:

$$\left(\frac{h\sigma}{\lambda}\right) = 0.55\, m \left(\frac{P}{H}\right)^{0.85} \qquad (7)$$

The above correlation differs slightly from the analytical result of Mikic and Rohsenow [7], but appears to be in better agreement with existing experimental information.

4. Acknowledgment

The author wishes to acknowledge the support of the Miller Institute for Basic Research in Science, University of California (Berkeley), through the appointment of Research Associate Professor during the year of 1967-1968.

5. References

[1] Clausing, A. M. and Chao, B. T., Thermal contact resistance in a vacuum environment, University of Illinois, Eng. Exp. Sta., Report ME-TN-242-1 (August 1963).

[2] Fried, E., Study of interface thermal contact conductance, NASA Document No. 64SD652 (May 1964).

[3] Yovanovich, M. M., Thermal contact conductance in a vacuum, Mech. Eng. Thesis, Mass Inst. Tech. (February 1966).

[4] Minges, L. M., Thermal contact resistance, Vol. I-A review of literature, Tech. Report AFML-TR-65-375, Air Force Materials Laboratory, Dayton, Ohio (April 1966).

[5] Clausing, A. M. and Chao, B. T., Thermal contact resistance in a vacuum environment, J. Heat Transfer 87C, 243 (1965).

[6] Yovanovich, M. M. and Fenech, H., Thermal contact conductance of nominally-flat, rough surfaces in a vacuum environment, Thermophysics and Temperature Control of Spacecraft and Entry Vehicles (Ed. G. B. Heller), Academic Press, New York (1966).

[7] Mikic, B. B. and Rohsenow, W. M., Thermal contact resistance, Tech. Rept. No. 4542-41, Dept. of Mech. Eng., Mass. Inst. Tech. (September 1966).

[8] Mikic, B. B., Yovanovich, M. M. and Rohsenow, W. M., The effect of surface roughness and waviness upon the overall thermal contact resistance, Tech. Rept. No. 76361-43, Dept. of Mech. Eng., Mass. Inst. Tech. (October 1966).

[9] Clausing, A. M., Heat transfer at the interface of dissimilar metals—the influence of thermal strain, Int. J. Heat Mass Transfer 9, 691 (1966).

[10] Laning, J. H., Jr. and Battin, R. J., Random Processes in Automatic Control, McGraw-Hill, New York (1956).

[11] Bennett, H. E. and Porteus, J. O., Relation between surface roughness and specular reflectance at normal incidence, J. Opt. Soc. Am. 51, 123 (1961).

[12] Kline, S. J., Similitude and Approximation Theory, McGraw-Hill, New York (1965).

[13] Weiss, V. and Gessler, J. G. (Eds.), Aerospace Structural Metals Handbook, Syracuse Univ. Press, Syracuse, New York (1963).

[14] Bloom, M. F., Thermal contact conductance in a vacuum environment, Missle and Space Systems Division, Douglas Aircraft Company Report SM-47700 (December 1964).

[15] Cunnington, G. R., Jr., Thermal conductance of filled aluminum and magnesium joints in a vacuum environment, ASME Paper No. WA/HT-40 (1964).

[16] Fried, E. and Atkins, H. Interface thermal conductance in a vacuum, J. Spacecraft and Rockets 2, 591 (1965).

[17] Fried, E. and Kelley, M. J., Thermal conductance of metallic contacts in a vacuum, Thermophysics and Temperature Control of Spacecraft and Entry Vehicles (Ed. G. B. Heller), Academic Press, New York (1966).

[18] Henry, J. J., Thermal contact resistance, Sc.D. Thesis, Mass. Inst. Tech. (August, 1964).

[19] Fumai, A. and Rolling, R. E., Inspection techniques for characterization of smooth, rough and oxidized surfaces, AIAA Paper No. 67-318, to appear in Thermophysics of Spacecraft and Planetary Bodies (Ed. G. B. Heller), Academic Press, New York (1967).

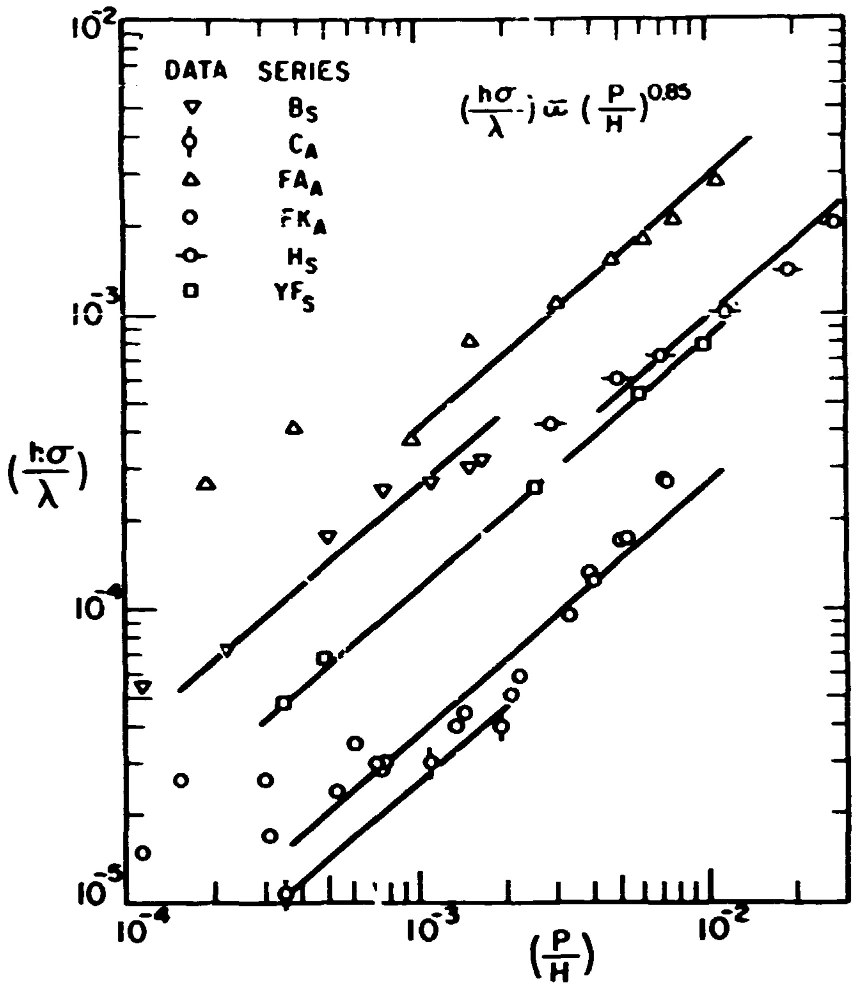

Figure 1. Thermal contact conductance for nominally-flat surfaces in a vacuum (data group 1).

Figure 2. Thermal contact conductance for nominally-flat surfaces in a vacuum (data group 2).